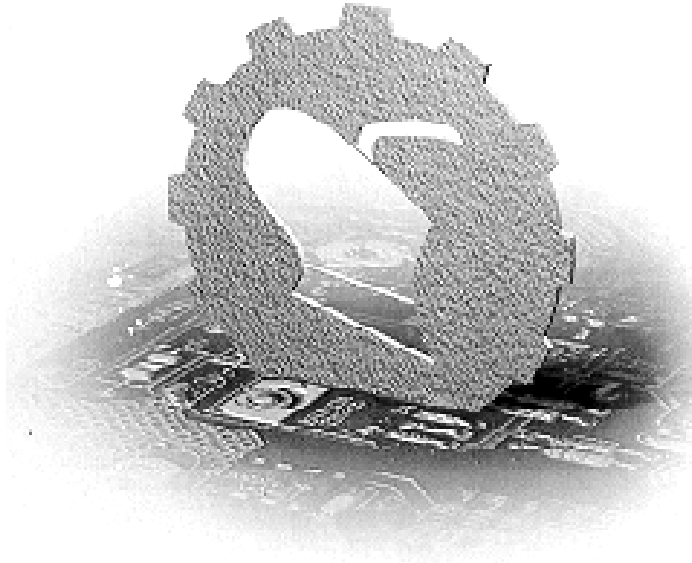


ISSN 0554-5587
UDK 631 (059)

ПОЉОПРИВРЕДНА ТЕХНИКА

AGRICULTURAL ENGINEERING

НАУЧНИ ЧАСОПИС
SCIENTIFIC JOURNAL



УНИВЕРЗИТЕТ У БЕОГРАДУ, ПОЉОПРИВРЕДНИ ФАКУЛТЕТ,
ИНСТИТУТ ЗА ПОЉОПРИВРЕДНУ ТЕХНИКУ

UNIVERSITY OF BELGRADE, FACULTY OF AGRICULTURE,
INSTITUTE OF AGRICULTURAL ENGINEERING



Година XXXIX Број 1, 2014.
Year XXXIX, No. 1, 2014.

Издавач (Publisher)

Универзитет у Београду, Польопривредни факултет, Институт за польопривредну технику,
Београд-Земун

University of Belgrade, Faculty of Agriculture, Institute of Agricultural Engineering, Belgrade-Zemun

Уредништво часописа (Editorial board)**Главни и одговорни уредник (Editor in Chief)**

др Горан Тописировић, професор, Универзитет у Београду, Польопривредни факултет

Уредници (National Editors)

др Ђукан Вукић, професор, Универзитет у Београду, Польопривредни факултет
др Стева Божић, професор, Универзитет у Београду, Польопривредни факултет
др Мирко Урошевић, професор, Универзитет у Београду, Польопривредни факултет
др Мићо Ољача, професор, Универзитет у Београду, Польопривредни факултет
др Анђелко Бајкин, професор, Универзитет у Новом Саду, Польопривредни факултет
др Милан Мартинов, професор, Универзитет у Новом Саду, Факултет техничких наука
др Душан Радивојевић, професор, Универзитет у Београду, Польопривредни факултет
др Драган Петровић, професор, Универзитет у Београду, Польопривредни факултет
др Раде Радојевић, професор, Универзитет у Београду, Польопривредни факултет
др Милован Живковић, професор, Универзитет у Београду, Польопривредни факултет
др Зоран Милеуснић, професор, Универзитет у Београду, Польопривредни факултет
др Рајко Миодраговић, доцент, Универзитет у Београду, Польопривредни факултет
др Александра Димитријевић, доцент, Универзитет у Београду, Польопривредни факултет
др Милош Пајић, доцент, Универзитет у Београду, Польопривредни факултет
др Бранко Радичевић, доцент, Универзитет у Београду, Польопривредни факултет
др Иван Златановић, доцент, Универзитет у Београду, Польопривредни факултет
др Милан Вељић, професор, Универзитет у Београду, Машински факултет
др Драган Марковић, професор, Универзитет у Београду, Машински факултет
др Саша Бараћ, професор, Универзитет у Приштини, Польопривредни факултет, Лешак
др Предраг Петровић, Институт "Кирило Савић", Београд
дипл. инг. Драган Милутиновић, ИМТ, Београд

Инострани уредници (International Editors)

Professor Peter Schulze Lammers, Ph.D., Institut fur Landtechnik, Universitat, Bonn, Germany

Professor László Magó, Ph.D., Szent Istvan University, Faculty of Mechanical Engineering, Gödöllő, Hungary

Professor Victor Ros, Ph.D., Technical University of Cluj-Napoca, Romania

Professor Sindir Kamil Okyay, Ph.D., Ege University, Faculty of Agriculture, Bornova - Izmir, Turkey

Professor Stavros Vougioukas, Ph.D., Aristotle University of Tessaloniki

Professor Nicolay Mihailov, Ph.D., University of Rousse, Faculty of Electrical Engineering, Bulgaria

Professor Silvio Košutić, Ph.D., University of Zagreb, Faculty of Agriculture, Croatia

Professor Selim Škaljić, Ph.D., University of Sarajevo, Faculty of Agriculture, Bosnia and Herzegovina

Professor Dragi Tanevski, Ph.D., "Ss. Cyril and Methodius" University in Skopje, Faculty of Agriculture, Macedonia

Professor Zoran Dimitrovski, Ph.D., University "Goce Delčev", Faculty of Agriculture, Štip, Macedonia

Professor Sitaram D. Kulkarni, Ph.D., Agro Produce Processing Division, Central Institute of Agricultural Engineering, Bhopal, India

Контакт подаци уредништва (Contact)

11080 Београд-Земун, Немањина 6, тел. (011)2194-606, 2199-621, факс: 3163-317, 2193-659,
e-mail: gogi@agrif.bg.ac.rs, жиро рачун: 840-1872666-79.

11080 Belgrade-Zemun, str. Nemanjina No. 6, Tel. 2194-606, 2199-621, fax: 3163-317, 2193-659,
e-mail: gogi@agrif.bg.ac.rs, Account: 840-1872666-79

ПОЉОПРИВРЕДНА ТЕХНИКА

НАУЧНИ ЧАСОПИС

AGRICULTURAL ENGINEERING

SCIENTIFIC JOURNAL

УНИВЕРЗИТЕТ У БЕОГРАДУ, ПОЉОПРИВРЕДНИ ФАКУЛТЕТ,
ИНСТИТУТ ЗА ПОЉОПРИВРЕДНУ ТЕХНИКУ
UNIVERSITY OF BELGRADE, FACULTY OF AGRICULTURE,
INSTITUTE OF AGRICULTURAL ENGINEERING

WEB адреса

www.jageng.agrif.bg.ac.rs

Издавачки савет (*Editorial Council*)

Проф. др Властимир Новаковић, Проф. др Милан Тошић, Проф. др Петар Ненић,
Проф. др Марија Тодоровић, Проф. др Драгиша Раичевић, Проф. др Ђуро Ерцеговић,
Проф. др Ратко Николић, Проф. др Драгољуб Обрадовић, Проф. др Божидар Јачинац,
Проф. др Драган Рудић, Проф. др Милош Тешић

Техничка припрема (*Technical editor*)

Иван Спасојевић, Пољопривредни факултет, Београд

Лектура и коректура: (*Proofreader*)

Гордана Јовић

Превод: (*Translation*)

Весна Ивановић, Зорица Крејић, Миљенко Шкрлин

Штампа (*Printed by*)

"Академска издања" – Земун
Часопис излази четири пута годишње

Тираж (*Circulation*)

350 примерака

Preplata za 2015. godinu iznosi 2000 dinara za institucije, 500 dinara za pojedince i 100 dinara za studente po svakom broju časopisa.

Радови објављени у овом часопису индексирани су у базама (*Abstracting and Indexing*):

AGRIS i SCIndeks

Издавање часописа помогло (*Publication supported by*)

Министарство просвете и науке Републике Србије

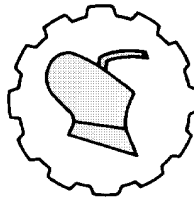
Na osnovu mišljenja Ministarstva za nauku i tehnologiju Republike Srbije po rešenju br. 413-00-606/96-01 od 24. 12. 1996. godine, časopis POLJOPRIVREDNA TEHNIKA je oslobođen plaćanja poreza na promet robe na malo.

S A D R Ž A J

NUMERIČKE SIMULACIJE TOPLITNIH OPTEREĆENJA TRAKTORISTE PROUZROKOVANIH SUNČEVIM ZRAČENJEM Dragan Ružić.....	1-8
UTICAJ RASPOREDA FERTIRIGACIJE I NAVODNJAVA VANA NA PORAST I PRINOS KRASTAVCA (<i>CUCUMIS SATIVUS L.</i>) Ashwini Patwardhan.....	9-14
POGODNOST ULJA PIRINČANIH MEKINJA KAO STOČNE HRANE ZA PROIZVODNNU BIODIZELA Abhinab Mishra, Ghanshyam Tiwari, Abhay Kumar Mehta, Sudhakar Jindal.....	15-20
UTICAJ DIJAGNOSTIKE STANJA NA POUZDANOST DVOSTRUKIH POLJOPRIVREDNIH KARDANSKIH VRTAILA Aleksandar N. Ašonja , Aleksandr Gennadievic Pastuhov.....	21-30
POREĐENJE KARAKTERISTIKA JEDNOG INDUKCIJONOG MOTORA, ČIJI PARAMETRI SU ODREĐENI EKSPERIMENTALNO I GENETIČKIM ALGORITMOM Anka Krasteva, Donka Ivanova, Miglena Hristova	31-38
REZULTATI ISPITIVANJA TEMPERATURE SOLARNIH MODULA Konstantin Koev, Krasimir Martev	39-47
POSTUPCI PAKOVANJA U MODIFIKOVANOJ ATMOSVERI RADI PRODUŽENJA VREMENA SKLADIŠTENJA KLICA LEBLEBIJA (<i>Cicer arietinum L.</i>) Ranjeet Singh, Ashok Kumar, Sitaram D. Kulkarni	49-59
UPOTREBA UNUTRAŠNJEGRADNJE NADPRITiska ZA Povećanje STABILNOSTI TANKOG ZIDA ROTACIONE SIMETRIČNE OPLATE OPTEREĆENE AKSIJALNOM SILOM Stanislav Kotšmíd, Marián Minárik.....	61-70

C O N T E N T S

NUMERICAL SIMULATION OF TRACTOR OPERATOR THERMAL LOADS CAUSED BY SOLAR RADIATION Dragan Ružić.....	1-8
EFFECT OF FERTIGATION AND IRRIGATION SCHEDULING ON GROWTH AND YIELD OF CUCUMBER (<i>CUCUMIS SATIVUS L.</i>) Ashwini Patwardhan.....	9-14
SUITABILITY OF RICE BRAN OIL AS FEEDSTOCK FOR BIODIESEL MAKING Abhinab Mishra, Ghanshyam Tiwari, Abhay Kumar Mehta, Sudhakar Jindal.....	15-20
THE INFLUENCE OF DIAGNOSTIC STATE OF RELIABILITY OF AGRICULTURE DOUBLE CARDAN SHAFT Aleksandar N. Ašonja, Aleksandr Genadievč Pastuhov.....	21-30
COMPARISON OF THE PERFORMANCE CHARACTERISTICS OF AN INDUCTION MOTOR, THE PARAMETERS OF WHICH ARE DETERMINED EXPERIMENTALLY AND BY A GENETIC ALGORITHM Anka Krasteva, Donka Ivanova, Miglena Hristova.....	31-38
RESULTS FROM A STUDY ON THE TEMPERATURE OF SOLAR MODULES Konstantin Koev, Krasimir Martev.....	39-47
MODIFIED ATMOSPHERIC PACKAGING STRATEGIES TO PROLONG SHELF LIFE OF CHICKPEA (<i>Cicer arietinum L.</i>) SPROUTS Ranjeet Singh, Ashok Kumar, Sitaram D. Kulkarni.....	49-59
INSIDE OVERPRESSURE UTILIZATION FOR A STABILITY INCREASING AT THE THIN-WALLED ROTATIONAL SYMMETRICAL SHELL STRAINED BY AXIAL FORCE Stanislav Kotšmíd, Marián Minárik.....	61-70



UDK: 629.06

*Originalni naučni rad
Original scientific paper*

NUMERICAL SIMULATION OF TRACTOR OPERATOR THERMAL LOADS CAUSED BY SOLAR RADIATION

Dragan Ružić*

*University of Novi Sad, Faculty of Technical Sciences, Department for Mechanization
and Design Engineering, Chair for Motor Vehicles and IC Engines,
Novi Sad, Serbia*

Abstract: This paper deals with analysis of solar radiation direction and intensity influence on thermal flux on agricultural tractor operator's body surface. The analysis was carried out on a virtual model of a tractor cab. The results showed that the highest solar load can occur when the sun is shining on the side of the tractor cab. When the sun is behind the cab and relatively low in the sky, the back and neck are critical body parts regarding the solar irradiation.

Key words: agricultural tractor cab, solar radiation, virtual thermal manikin, CFD, thermal comfort

INTRODUCTION

Thermal conditions in agricultural tractor cab are more adverse in hot than in cold ambient. Higher ambient temperatures, accompanied with solar radiation, cause increase of both interior air and surface temperatures above safety limits. From that reason, although the tractor cab offers the mechanical protection and protection from adverse ambient conditions, on the other hand, even under moderate outside conditions the closed cab act like green house and its closed interior could become unpleasant, unbearable and even dangerous.

* Corresponding author. E-mail: ruzic@uns.ac.rs

Project TR31046 "Improvement of the quality of tractors and mobile systems with the aim of increasing competitiveness and preserving soil and environment", supported by Serbian Ministry of Education, Science and Technological Development

Experimental determination of local heat fluxes on human body surface caused by solar radiation demands the use of complex and expensive measurement equipment and test facilities. The other way is to simulate these processes in virtual experiments, as in other fields of research [3], [5]. This paper deals with numerical modelling of solar radiation transmitted through tractor cab glazing.

Number of researches is focused on person thermal load caused by solar radiation, and this problem is especially interesting in field of mobile machinery. An operator enclosure can be treated as a workspace and the conditions inside a tractor cab have significant impact on the performance of the operator. From the operator's point of view, tractor cab ergonomics is a key factor in ensuring his optimum working performance, which could easily become the weakest link in the working process.

The project presented in the report by Bohm *et al.* [1], concerns the thermal effect of glazing in cabs with large glass areas. The effect of different kind of glass and design of the windows as well as the effects of sun protection and insulation glazing have been studied and evaluated, using the thermal manikin called AIMAN. Results showed that neither in severe winter conditions, nor in sunny summer conditions, could acceptable climate be obtained with standard glazing in cabs with large glass areas.

In the comprehensive project focused on the reduction of vehicle auxiliary load, done by National Renewable Energy Laboratory [7], variety of researching methods were used to research and develop innovative techniques and technologies for lowering thermal loads. The aim of the research was to investigate solutions for improvement of fuel economy of air-conditioning system. They concluded that reflecting the solar radiation incident on the vehicle's glass is the most important factor in making significant reductions in the thermal loads. Using solar-reflective glass can reduce the average air temperature and the seat temperature. Using reflective shades and electrochromic switchable glazing is also effective techniques for reducing the solar energy entering the passenger compartment. They also found that solar-reflective coatings on exterior opaque surfaces and body insulation can reduce a vehicle's interior temperatures, but to a lesser extent than solar-reflective glazing, shades, and parked-car ventilation can.

Results of Ružić *et al.* [8], [9], [10] showed that tractor cab glazing is the most influencing factor for thermal loads. They concluded that the highest heat flux that enters the cab is caused by solar radiation through the glass, which could be several times higher than the heat transferred by other modes. Therefore, the selection of appropriate glass properties could be the way to reduce operator's thermal load. Furthermore, the shape of a cab, glass solar properties and thermal load of the operator are in close relation.

The aim of the paper is to investigate influence of sun position relative to the tractor cab on heat fluxes caused by solar radiation over the operator's body surface. Furthermore, the goal is to identify the worst case regarding solar heat load, since the exposed surfaces of the body must be either protected from the adverse effects of solar radiation or directly cooled by airflow from air-conditioner vents, in order to reduce risk of thermal discomfort.

MATERIAL AND METHODS

Determination of heat fluxes caused by solar radiation was done using the numerical simulations. The simulations were carried out in STAR CCM+ software. The CAD model of the virtual thermal manikin (VTM) is a simplified humanoid in the sitting

posture. The manikin's body is symmetric, with its posture defined by characteristic points in places where the main body joints are (hips, shoulders, neck, elbows etc). Main body dimensions are adopted from CATIA database for a 50th percentile European male, and the body is divided into 18 segments (Fig. 1). According to the chosen sizes of the body, the VTM is 1.74 m tall and weighs 68 kg. The area of VTM body surface in sitting position is 1.796 m². The VTM surface is discretized in around 13,600 surface elements.

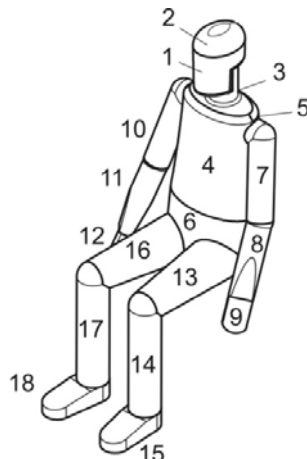


Figure 1. Virtual thermal manikin with numbered segments

The cab was modelled after the protective operator's cab of small agricultural tractor powered by 30 kW engine. The interior geometry was simplified, neglecting non-important and small details such command levers etc.

The amount of solar radiation energy that will be absorbed by the body will depend on the effective projected area and on the solar absorptivity of the body surface. The largest effective projected radiation area A_{eff} of a person in the sitting position is with the azimuth and altitude angles of 30° and 15° respectively [2], [6]. Solar absorptivity of the human skin is around 0.62, while solar absorptivity for clothing depends on the colour [4], [6]. In this research, solar absorptivity of all virtual manikin's segments was set to 0.62.

The problem was treated as a steady-state three-dimensional, with stationary bodies and boundaries. Solar load was calculated by *Solar load model* incorporated in CFD software STAR-CCM+. The coordinate system for the orientation of the direct solar flux is defined in the Fig. 2. In this study, the gray spectrum model is used and the total solar loads represent the full-thermal spectrum, including both direct and diffuse components. The solar load model is defined by the following properties: the sun direction vector in a specified coordinate system (azimuth and altitude angles), the direct and the diffuse solar fluxes (W·m⁻²) [15].

Solar irradiation is variable depending on the position of the sun as well as the orientation of the cab. Fig. 3 presents the values of maximum ("clear sky") intensity of normal irradiation and its variations during the daylight, in a central European region.

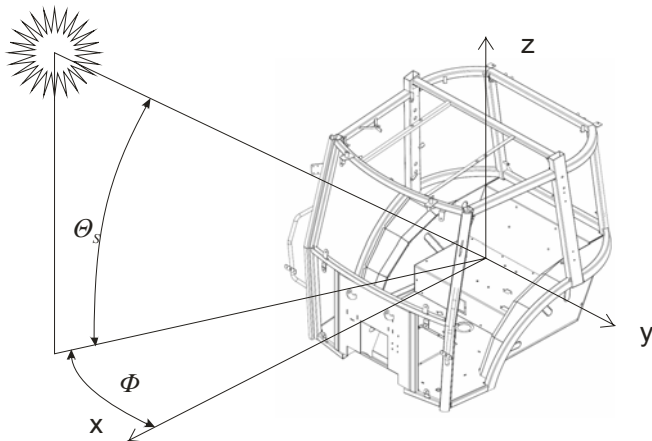


Figure 2. Solar coordinate system relative to tractor cab:
 θ_S – solar altitude (sun elevation), Φ - azimuth angle

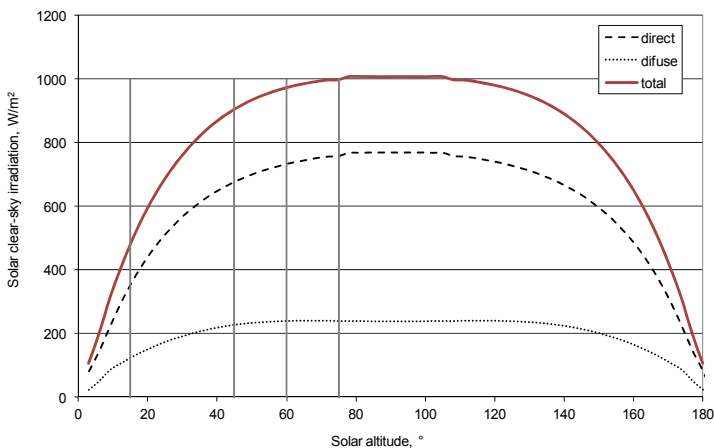


Figure 3. Solar clear-sky irradiation in a central European region on a day in July
(<http://re.jrc.ec.europa.eu/pvgis/apps3/pvest.php>).

Vertical lines present the solar altitudes that were considered in the analysis

Tractor cab glazing is semi-transparent medium where solar irradiation can be partially reflected, absorbed and transmitted. Absorbed part of the solar energy will be emitted to the cab interior by both convection and long-wave radiation. When a tractor cab is exposed to the sun, the operator's body receives the heat partly by solar radiation transmitted through the glass and partly by long-wave thermal radiation from the surrounding surfaces. Total amount of heat transmitted through the glass caused by solar radiation is related with cab surface projection normal to the radiation direction.

In this research, only transmitted part of the solar radiation was analyzed, since it has direct effect on the operator, increasing his skin temperature and hence producing the discomfort. Using available values of glass properties for tinted glass (green, with 75% transmittance of visible light [14]) normal solar transmissivity was set to 0.5.

RESULTS AND DISCUSSION

The aim of the research is to investigate influence of sun position relative to the tractor cab on heat fluxes caused by solar radiation over the body surface. This mode of heat load is independent of other boundary conditions parameters, like ambient temperature, air velocity or radiant temperature.

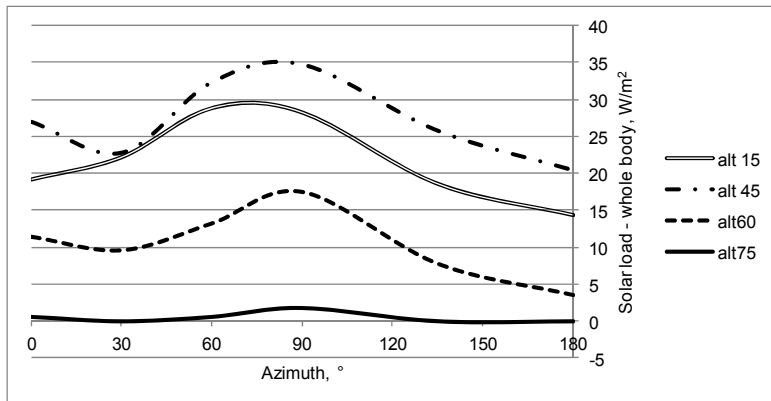


Figure 4. Values of the heat flux for the whole body
in dependence of solar azimuth and altitude angles

Relevant standards for investigation of thermal conditions in tractor cabs do not define solar load during the tests of air-conditioning system [12]. Therefore, in order to find the worst case, simulations were performed for four different sun altitudes ($\theta_S = 15^\circ, 45^\circ, 60^\circ$ and 75°) and six azimuth angles ($\phi = 0^\circ, 30^\circ, 60^\circ, 90^\circ, 135^\circ$ and 180°). The azimuth angles covered only the one half of the cab due to its longitudinal symmetry. Direct and diffuse solar irradiation were changed with sun altitude, according to the graph in Fig. 3. The sun position angles were including the direction when the largest area of body in sitting position is exposed to the radiation ($\theta_S = 15^\circ$ and $\phi = 30^\circ$), as mentioned above.

Values of the heat flux for the whole body in dependence of solar azimuth and altitude angles are shown on graph in Fig. 4. The highest heat flux averaged for the whole body was achieved for azimuth angle 90° and altitude 45° . Distribution of the heat flux on VTM's surface is visualized on Fig. 5 and values are given on graph in Fig. 6. It can be noted strong asymmetry of thermal loads on the operator's body.

The operator's head is well protected and is exposed only when the sun is low in the sky, i.e. altitude is around 15° . However, under this circumstance solar irradiation is approximately one-half of its maximum value. The segment with the highest heat flux is operator's back, for cases where the sun is behind the cab and relatively low in the sky (the sun altitude between 15 and 45°), graph in Fig. 7. When the sun is high in the sky (around the noon), the cab roof offers relatively good protection for the whole body.

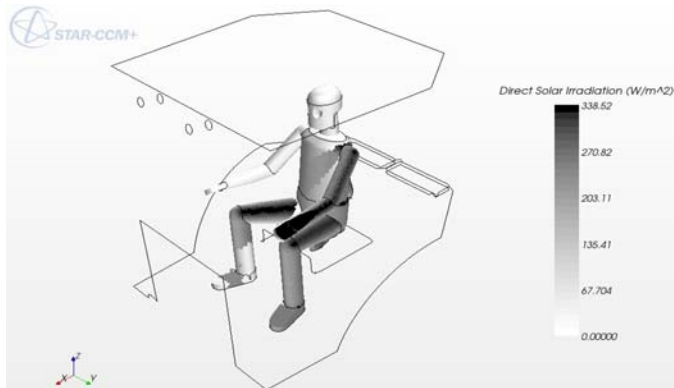


Figure 5. Distribution of solar heat load over the VTM's surface in the case with the highest heat flux for the whole body

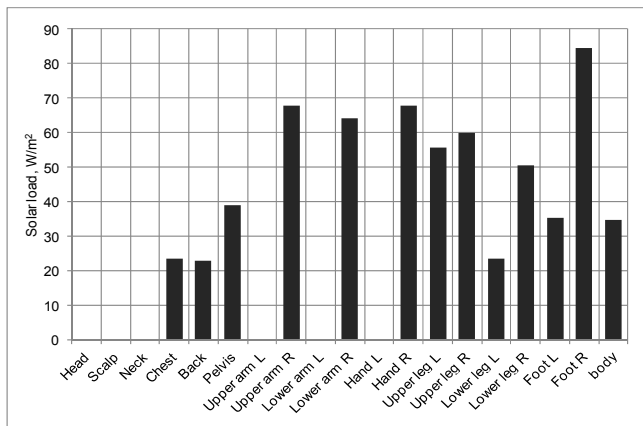


Figure 6. Values of solar load heat flux on VTM's segments in the case with the highest heat flux for the whole body

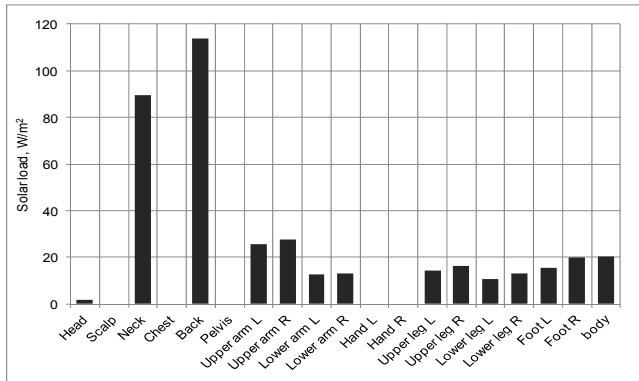


Figure 7. Values of solar load heat flux on VTM's segments when the sun is behind the cab and at altitude of 45°

CONCLUSION

Tractor cab design and the operator's position on the seat generally do not offer good protection from solar radiation, although roof ensures shading for the operator under some circumstances. The highest heat flux that the body receives is when the sun is shining on the side of the tractor cab. The back and neck are critical body parts regarding the solar irradiation, when the sun is behind the cab and relatively low in the sky. When the sun is low in the sky, the head and the trunk are exposed and protected only by solar properties of glass, unless some kind of solar shading devices or direct cooling by air-conditioning are used.

Shading devices can be placed on the inner side, or as a better solution, on the outer side of the cab. In both cases, the shading devices must not restrict the operator's normal field of vision in the working area of the tractor. For that reason, sun visors or curtains must be easily adjustable. In addition to shading the operator, the outer shading devices prevent increase of temperature of glass and other surfaces caused by the solar radiation. A common solution for these purposes is the use of cab roof overhangs, since aerodynamics is not an issue in agricultural tractors. Furthermore, paying attention to solar characteristics of glass and design of air distribution system in such way that air-conditioner vents can be directed to areas with the highest fluxes are an efficient way to reduce the operator's thermal load.

Numerical values obtained from the simulations should be considered for comparison purposes only, and validation of the numerical model must be done by experiment on physical models.

REFERENCES

- [1] Bohm, M., Holmer, I., Nilsson, H., Noren, O. 2002. *Thermal effects of glazing in driver's cabs*, JTI-rapport 305, JTI – Institutet for jordbruks, ISSN 1401-4963, Uppsala, Sweden
- [2] Fanger, P. O. 1970. *Thermal Comfort*, Copenhagen, Denmark: McGraw-Hill,
- [3] Glišović, J., Demić, M., Miloradović, M. 2011. Review of Virtual Reality Applications for Reducing Time and Cost of Vehicle Development Cycle. *Journal of Applied Engineering Science* Vol 9(3): 361-372
- [4] Incropera, F. P., DeWitt, D. P. 1981. *Fundamentals of Heat and Mass Transfer*, New York, USA: John Wiley & Sons
- [5] Ognjanović, M. 2008. Design in Mechanical Engineering - Multidisciplinary Approach. *Istraživanja i projektovanja za privredu*, 20/2008: 15-22
- [6] Parsons, K. 2003. *Human thermal environments: The effects of hot, moderate and cold environments on human health, comfort and performance*, 2nd Edition. London, UK: Taylor & Francis
- [7] Rugh, J. & Farrington, R. 2008. *Vehicle Ancillary Load Reduction Project Close-Out Report*, Technical Report NREL/TP-540-42454, Golden, USA: National Renewable Energy Laboratory
- [8] Ružić, D., Časnji, F. 2011. Konstruktivni parametri kabine od uticaja na toplotnu interakciju između čoveka i kabine. *Poljoprivredna tehnika*, 36 (1): 11-19
- [9] Ružić, D., Časnji, F. 2012. Thermal interaction Between a Human Body and a Vehicle Cabin, published in: *Heat Transfer Phenomena and Applications*, S. N. Kazi (ed.), InTech
- [10] Ružić, D., Časnji, F., Muzikravić V. 2007. Karakteristike stakla kao faktor od uticaja na mikroklimu u traktorskoj kabini. *Traktori i pogonske mašine*, 12 (4): 92-97

- [11] Türler, D., Hopkins, D., Goudey, H. 2003. Reducing Vehicle Auxiliary Loads Using Advanced Thermal Insulation and Window Technologies. *SAE Paper 03HX-36*, USA: Society of Automotive Engineers
- [12] ***. 1997. ASABE/ISO 14269-2 Tractors and Self-propelled Machines for Agriculture and Forestry - Operator Enclosure Environment - Part 2: Heating, Ventilation and Air-conditioning Test Method and Performance
- [13] ***. 1999. *ASHRAE Book of Applications, Chapter 32: Solar Energy Use*, American Society of Heating, Refrigerating and Air Conditioning Engineers, Atlanta, USA
- [14] ***. 2003. *Saint-Gobain Sekurit - Glazing Manual*, available at <http://www.sekurit.com>, [accessed at july 2013]
- [15] ***, *STAR-CCM+, User Guide*, CD-Adapco, 2011

NUMERIČKE SIMULACIJE TOPOLTNIH OPTEREĆENJA TRAKTORISTE PROUZROKOVANIH SUNČEVIM ZRAČENJEM

Dragan Ružić

*Univerzitet u Novom Sadu, Fakultet tehničkih nauka, Departman za mehanizaciju
i konstrukciono mašinstvo, Katedra za motore i vozila, Novi Sad*

Sazetak: U radu je prikazana analiza uticaja pravca i intenziteta sunčevog zračenja na toplotni fluks na površini tela rukovaoca u kabini poljoprivrednog traktora. Analiza je izvršena na virtuelnom modelu kabine. Rezultati su pokazali da najveće toplotno opterećenje tela usled sunčevog zračenja može nastati kada je kabina bočnom stranom okrenuta ka suncu, a da je najveće lokalno toplotno opterećenje na leđima i na vratu rukovaoca kada je sunce iza kabine.

Ključne reči: *traktorska kabina, sunčev zračenje, virtuelna toplotna lutka, CFD, toplotni komfor*

Prijavljen: 16.8.2013

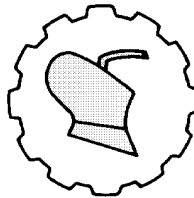
Submitted:

Ispravljen:

Revised:

Prihvaćen: 07.10.2013.

Accepted:



UDK: 634.11

*Originalni naučni rad
Original scientific paper*

EFFECT OF FERTIGATION AND IRRIGATION SCHEDULING ON GROWTH AND YIELD OF CUCUMBER (*CUCUMIS SATIVUS L.*)

Ashwini Patwardhan*

*K. K. Wagh College of Agricultural Engineering, Department of Irrigation and
Drainage Engineering, Nashik, Affiliated to Mahatma Phule Krishi Vidyapeeth,
Rahuri, India*

Abstract: The maximum yield ($21.67 \text{ t}\cdot\text{ha}^{-1}$ and $20.85 \text{ t}\cdot\text{ha}^{-1}$) was obtained with fertigation level F_1 (80% of R.D) and irrigation level I_2 (0.3PE). The yield was 44.28% and 39% higher in fertigation level F_1 and irrigation level I_2 as compared to conventional method of irrigation. The individual effect of fertigation and irrigation levels showed significant effect on the yield but the interaction effect between fertigation and irrigation levels was found to be non-significant. The maximum water use efficiency (WUE) of $11.6 \text{ t}\cdot\text{ha}^{-1}\cdot\text{mm}$ and $10.9 \text{ t}\cdot\text{ha}^{-1}\cdot\text{mm}$ was recorded with I_1 and F_1 while maximum fertilizer use efficiency (FUE) of 135.10 was recorded with F_1 . The total quantity of water applied through drip irrigation and conventional method of irrigation was 16.35 cm and 48.00 cm respectively, indicating 65.93% saving of water in drip irrigation system over conventional method of irrigation. The B:C ratio 1.94 was found maximum in treatment combination $I_2 F_1$.

Key words: cucumber, irrigation, water use efficiency, fertilizer use efficiency, fertigation, yield, B:C ratio.

INTRODUCTION

Cucumber has high place in the diet as a rich source of carbohydrates, as a breakfast fruit and as an ingredient of salads. Cucumber forms an important and big group of vegetable in our diet due to its high nutritive value (44.5 g of average nutritive value per

* Corresponding author. E-mail: satputeaa@yahoo.co.in

100 g dry matter). It can give cool and refreshing effects in summer. The area and productivity of cucumber is very low in Maharashtra. Hence to increase the production per unit use of water, adequate and timely supply of water is crucial one. The important input which seriously affects the growth and yield of any vegetable is fertilizer application. Thus with Hi-tech irrigation practice like drip irrigation, fertilizer were applied with water directly in the root-zone of crop, thereby avoiding leaching and percolation losses with the economy in the use of fertilizers and water to be applied. The cultural practices coupled with balanced use of fertilizers and optimum use of irrigation water plays an important role in enhancing the productivity of cucumber. Therefore the present study was aimed to work out fertilizer and water requirement, compare yield of cucumber, *WUE* and *FUE* as influenced by drip and surface irrigation method and compute benefit cost ratio.

MATERIAL AND METHODS

The field experiment was conducted at the Instructional Farm of Department of Irrigation and Drainage Engineering, Dr. Annasaheb Shinde College of Agricultural Engineering, MPKV., Rahuri on clay soil during the period from December 2004 to March 2005. The topography of the experimental field was uniform and leveled. The EC and pH of the experimental plot were 0.502 dSm^{-1} and 8.05, respectively. Available N, P and K were observed as $416.97 \text{ kg}\cdot\text{ha}^{-1}$, $45.824 \text{ kg}\cdot\text{ha}^{-1}$, $728.00 \text{ kg}\cdot\text{ha}^{-1}$. The quality of water was of class C_3S_1 .

The experiment was carried out in split plot design with three main-plot treatments and four sub-plot treatments with one control treatment each having three replications. The main-plot treatments included I_1 : Irrigation at 0.2PE by drip irrigation method, I_2 : Irrigation at 0.3PE by drip irrigation method, I_3 : Irrigation at 0.4PE by drip irrigation method, Where 0.2, 0.3 and 0.4 were the integrated factors derived from crop coefficient (K_c), pan factor (K_p) and wetted area (W_a). Sub-plot treatments included F_1 : 80% of recommended dose (*RD*) through water soluble fertilizer (*WSF*), F_2 : 100% of recommended dose through water soluble fertilizer, F_3 : 120% of recommended dose through water soluble fertilizer and F_4 : Application of N through drip and P, K by band placement according to recommended dose. The treatments were compared with a suitable control i.e with conventional method of irrigation (ridges and furrows) replicated thrice.

The experiment was laid out with twelve treatment combinations arranged randomly on a field of $40 \text{ m} \times 22 \text{ m}$ size with spacing of $1.0 \text{ m} \times 0.5 \text{ m}$ while with conventional method of irrigation on a field of $40 \text{ m} \times 1 \text{ m}$ size with a spacing of $0.5 \text{ m} \times 1.0 \text{ m}$. The buffer of 1m was left between two successive treatment plots in order to avoid lateral movement of water from one treatment plot to another. One lateral commanded two rows of cucumber plants. The seeds of cucumber (var. Himangi) were dibbled on 29th December 2004 at the rate of $1.50 \text{ kg}\cdot\text{ha}^{-1}$.

Water-soluble fertilizer (Ultrasol) of grade (19:19:19) and urea was used for treatments with fertigation levels from F_1 to F_3 while urea (46% N), single super phosphate (16% P_2O_5), murate of potash (60% K_2O) were used for treatment with fertigation level F_4 and conventional method of irrigation. The recommended dose of fertilizer (NPK) for the cucumber crop is $100:50:50 \text{ kg}\cdot\text{ha}^{-1}$. Water soluble fertilizers

(Ultrasol) were applied weekly as per different treatments. The basal dose was divided into four splits as 10%, 30%, 30% and 30% respectively and was applied weekly after sowing, whereas the dose for top dressing was divided into four equal splits as 12.5% and was applied weekly in the next month.

In case of control, solid fertilizers were used in which half dose of N and full dose of P and K were given at the time of sowing and remaining half dose of N was given one month after sowing.

The effect of fertigation and irrigation levels on growth and yield contributing parameters viz., length of vine, diameter of fruit, weight of fruit, length of fruit, number of fruit, compactness of fruit and yield of fruit were observed.

RESULTS AND DISCUSSION

It was observed that the maximum 480.00 mm depth of irrigation water was applied to cucumber crop in control treatment followed by 227.04, 195.28 and 163.52 mm as in irrigation level I_3 , I_2 , I_1 that was 237.04 mm respectively through drip irrigation system. The maximum saving (65.58%) of water in I_1 was achieved with drip irrigation system over control.

It was also observed that the yield per hectare of cucumber differed significantly due to irrigation levels. The maximum average yield of 20.83 t-ha^{-1} was reported for treatment I_2 (0.3PE) and was found significantly superior over rest of treatments (I_1 and I_3). This might be due to the favorable moisture status in the rootzone of crop produced by treatment with irrigation level I_2 during the growth period as compared to treatment with I_1 (0.2PE) and I_3 (0.4PE), which resulted in reduced average yield of fruit. The treatments I_1 and I_3 were at par with each other. The minimum yield of 17.79 t-ha^{-1} was observed in irrigation level of I_3 . Similarly, it was revealed that the average yield per hectare of cucumber varied significantly due to fertigation levels. The maximum average yield of 21.62 t-ha^{-1} was obtained in treatment F_1 (80% R.D) and was significantly superior over F_3 and F_4 . The treatment F_1 and F_2 were at par with each other. However the average yield obtained in F_2 was significantly superior to that obtained by F_4 (N through drip and P, K by band placement) and was also at par with F_3 . It was also reported that average yield obtained in treatment F_3 was at par with F_4 . The interaction effect between irrigation levels and fertigation levels was observed to be non-significant in respect of average yield per hectare. In control treatment, the minimum average yield of 14.98 t-ha^{-1} was registered, this decrease in yield in case of control treatment might be caused due to deep percolation and conveyance losses of fertilizers during application.

From Tab. 1. it was revealed that the *WUE* ranged from $3.12 \text{ t-ha}^{-1}\text{-mm}$ to $11.6 \text{ t-ha}^{-1}\text{-mm}$ due to different treatments. It was revealed that maximum WUE was reported in treatment with irrigation level I_1 (0.2PE) and with fertigation level F_1 (80% RD). The increase in *WUE* was largely due to reduction in total water used. It was also noted that through drip system maximum *WUE* was achieved than with conventional method of irrigation. The saving in irrigation water was to the extent of 63.12% and 59.32% [2] in case of irrigation level I_1 (0.2PE) and I_2 (0.3PE) in drip irrigation system as compared with conventional method of irrigation. In other words, within the same quantity of water, about 63.12% and 59.32% additional area could have been brought under irrigation.

Table 1. Water and fertilizer use efficiency as influenced by different treatment

Treatments	Yield [t·ha ⁻¹]	Depth of water applied [cm]	Water use efficiency [t·ha ⁻¹ -mm]	Percent saving in water [%]	Quantity of fertilizer applied [kg·ha ⁻¹]	Fertilizer use efficiency [%]	Increase in yield [%]
<i>Irrigation levels</i>							
I_1	18.94	16.35	11.6	65.93	200	94.71	20.91
I_2	20.83	19.83	10.7	59.32	200	104.13	28.06
I_3	17.79	23.70	7.5	50.61	200	88.96	15.74
<i>Fertigation levels</i>							
F_1	21.62	19.86	10.9	58.62	160	135.10	30.69
F_2	19.86	19.86	10.0	58.62	200	99.30	24.56
F_3	18.44	19.86	9.3	58.62	240	76.81	18.73
F_4	16.84	19.86	8.5	58.62	200	84.18	11.02
<i>Control</i>	14.98	48.00	3.1	-	200	74.91	-
		<i>Irrigation levels</i>		<i>Fertigation levels</i>		<i>Interaction (Ix F)</i>	
<i>SE ±</i>		2.29		6.78			
<i>CD at 5%</i>		9.02		20.14		N.S.	

The maximum value of FUE (135.10%) was observed in Tab. 1 for fertigation level with F_1 (80% RD) followed by F_2 (100% RD), F_3 (120% RD) and F_4 (N through drip and P, K by band placement) whereas in case of irrigation levels FUE was observed maximum (104.17%) in I_2 (0.3PE) followed by I_1 (0.2PE) and I_3 (0.4PE). The drip irrigation treatment registered maximum values of FUE as compared to those obtained with conventional method of irrigation. It was revealed that there was 30.69% increase in yield and 20% saving in fertilizers over control.

Table 2. Cost economics of fertigation for different treatments

Items	I_1F_4	I_1F_2	I_1F_1	I_1F_3	I_2F_2	I_2F_3	I_2F_1	I_2F_4	I_3F_3	I_3F_1	I_3F_4	I_3F_2	Control
<i>Cost of production [Rs·ha⁻¹]</i>	40257	49881	47420	52293	49881	52293	47420	40257	52293	47420	40257	49882	
<i>Gross monetary return [Rs]</i>	65600	80000	86400	70400	62700	82800	92000	74400	67600	80400	61600	59600	
<i>Net income [Rs]</i>	23343	30119	38980	18107	12819	30507	44580	15307	22980	24518	21343	25873	
<i>B:C Ratio</i>	1.63	1.60	1.82	1.35	1.28	1.58	1.94	1.85	1.29	1.70	1.53	1.49	1.76

The maximum B:C ratio was observed in treatment combination I_2F_1 (1.94) and the least value was found in treatment combination I_2F_2 (1.28) for drip irrigation system whereas it was 1.76 in control (Tab. 2).

Cost of production ($\text{Rs}\cdot\text{ha}^{-1}$) = seasonal fixed cost Rs.8890/-, Variable and fertilizer cost, rental value $\text{Rs. } 1000\cdot\text{ha}^{-1}$ and interest on working capital 10%, selling price $\text{Rs. } 400\cdot\text{q}^{-1}$. The study revealed that there was 30.69% increase in yield and 20% saving in fertilizers over control. The highest water use efficiency ($11.58 \text{ t}\cdot\text{ha}^{-1}\cdot\text{mm}$) was found in treatment with irrigation level I_1 (0.2PE) whereas in case of fertigation level highest value of WUE ($10.9 \text{ t}\cdot\text{ha}^{-1}\cdot\text{mm}$) was recorded in F_1 (80% RD). The fertilizer use efficiency was recorded highest (104.13%) in irrigation level I_2 (0.3PE) whereas in case of fertigation level highest value (135.10%) was recorded for F_1 (80% RD). The maximum B:C ratio (1.94) was found in treatment combination I_2F_1 which was the combination of treatments with irrigation level I_2 (0.3PE) and fertigation level F_1 (80% RD) with the maximum net income of 44,580 $\text{Rs}\cdot\text{ha}^{-1}$.

CONCLUSIONS

From the present study it was concluded that though the effect of interaction between irrigation and fertigation level was found statistically non-significant but the individual effects of irrigation and fertigation levels gave significant results. Thus, it was concluded that cucumber irrigated with 0.3PE grown in clay soil with irrigation scheduled on the alternate day, and with 80% of RD through WSF showed better results in respect of yield under Rahuri conditions.

BIBLIOGRAPHY

- [1] Narayananamoothy, A. 1997. Economic viability of drip irrigation: An Empirical Analysis from Maharashtra. *India Journal of Agricultural Economics*, Vol.52, No.4, October-December, pp.728-739.
- [2] NCPAH. 2001. *Progress report*. Ministry of Agriculture, Government of India, New Delhi.
- [3] Pollack, S. 1995. *Cucumbers: An Economic Assessment of the Feasibility of Providing Multiple-Peril Crop Insurance*. Economic Research Service, USDA, pp-15-19.

UTICAJ RASPOREDA FERTIRIGACIJE I NAVODNJAVA VANJA NA PORAST I PRINOS KRASTAVCA (*CUCUMIS SATIVUS L.*)

Ashwini Patwardhan

K. K. Wagh Fakultet za poljoprivrednu tehniku, Institut za navodnjavanje i odvodnjavanje, Nashik, Rahuri, Indija

Sažetak: Maksimalni prinos ($21.67 \text{ t}\cdot\text{ha}^{-1}$ i $20.85 \text{ t}\cdot\text{ha}^{-1}$) je postignut sa nivoom fertirigacije F_1 (80% R.D) i nivoom navodnjavanja I_2 (0.3PE). Prinos je bio 44.28% i

39% viši sa nivoom fertirigacije F_1 i nivoom navodnjavanja I_2 u poređenju sa konvencionalnom metodom navodnjavanja. Pojedinačni efekti nivoa fertirigacije i navodnjavanja pokazali su značajan uticaj na prinos, ali efekat interakcije nivoa fertirigacije i navodnjavanja nije bio značajan. Maksimalna efikasnost navodnjavanja (WUE) od $11.6 \text{ t}\cdot\text{ha}^{-1}\cdot\text{mm}$ i $10.9 \text{ t}\cdot\text{ha}^{-1}\cdot\text{mm}$ je postignuta sa I_1 i F_1 dok je maksimalna efikasnost đubrenja (FUE) od 135.10 postignuta sa F_1 . Ukupna količina vode koja je upotrebljena za navodnjavanje kap po kap i konvencionalni metod navodnjavanja bila je 16.35 cm i 48.00 cm , redom, pokazujući uštedu vode od 65.93% pri navodnjavanju kap po kap u odnosu na konvencionalni metod navodnjavanja. Odnos B:C od 1.94 je bio maksimalan u tretmanu kombinacijom nivoa $I_2 F_1$.

Ključne reči: krastavac, navodnjavanje, efikasnost navodnjavanja, efikasnost đubrenja, fertirigacija, prinos, odnos B:C

Prijavljen: 31.8.2013

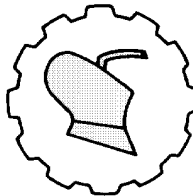
Submitted:

Ispravljen: 10.3.2014.

Revised:

Prihvaćen: 15.3.2014.

Accepted:



UDK: 547.916

*Originalni naučni rad
Original scientific paper*

SUITABILITY OF RICE BRAN OIL AS FEEDSTOCK FOR BIODIESEL MAKING

Abhinab Mishra^{1*}, Ghanshyam Tiwari¹, Abhay Kumar Mehta¹, Sudhakar Jindal²

¹*Maharana Pratap University of Agriculture and Technology, College of Technology and Engineering, Department of Farm Machinery and Power Engineering, Udaipur, India*

²*Maharana Pratap University of Agriculture and Technology, College of Technology and Engineering, Department of Mechanical Engineering, Udaipur, India*

Abstract: India is second largest rice producing country and the estimated yield of crude rice bran oil (RBO) is about 400.000 tons of which only 50% is of edible grade, 50% of the total available rice bran oil is left unutilized due to presence of active lipase in bran and lack of economic stabilization methods most of the bran is used as animal feed or for industrial application. One of the best ways for the potential utilization of RBO is the production of biodiesel; also a very little research has been done to utilize this oil as a replacement for mineral diesel. In the present study, biodiesel has been prepared from Rice Bran oil by trans-esterification method meeting the acceptable quality standards and then used as fuel.

Key words: *rice bran oil, blend, trans-esterification, biodiesel*

INTRODUCTION

Energy is an essential requirement for economic and social development for any country but, with advent of industrial revolution and sky rocketing of petroleum fuel costs in present day has led to growing interest in alternative fuels which can be produced from locally available resources within the country such as alcohol, biodiesel, vegetable oils etc in order to provide a suitable substitute to diesel for a compression ignition (CI) engine [1, 5]. Presently the vegetable oils are the promising alternative fuel to diesel oil since they are renewable, biodegradable and clean burning fuel having similar properties as that of diesel.

* Corresponding author. E-mail: abhinab_mishra@yahoo.com

The most commonly used method to make vegetable oil suitable for use in CI engines is to convert it into biodiesel. Some of the vegetable oils like jatropha, karanj, sunflower, and castor are converted into biodiesel for a substitute to diesel for compression ignition (CI) engine but unavailability of these oils in plenty amount, rice bran oil may be one of the option. The estimated yield of crude rice bran oil (RBO) in our country is about 400.000 tons of which only 50% is of edible grade, 50% of the total available rice bran oil is left unutilized due to presence of active lipase in bran, which hydrolyses the triglyceride to fatty acids and glycerol, as a result the FFA content increases making difficult to refine, due to the presence of tightly associated wax [6]. Hence, the oil has to be de-waxed and degummed before being neutralized which lack economic stabilization. As a result most of the bran is used as animal feed or for industrial application. One of the best ways for the potential utilization of RBO is to extract Biodiesel from it; also a very little research has been done to utilize this oil as a replacement for mineral diesel.

MATERIAL AND METHODS

Filtration of crude oil

The crude rice bran oil was procured and various samples were prepared. The oil was filtered to remove the contaminants of oil to obtain a clear biodiesel. Due to excess viscosity and contaminants in the oil a filtration unit was made in which the oil was filtered from a filter cloth of 5 micron with a vacuum pump to obtain clear oil for the experiment (Fig.1).



Figure 1. Filtration unit

Determination of free fatty acid content

The clear filtered oil was further processed for esterification process for obtaining biodiesel. Before esterification process it is very important to determine the free fatty acid content of the oil. In order to determine the percent of FFA content in the oil,

chemical titration method was adopted as per manual of methods of analysis of foods, oils, and fats, Directorate General of health Services, Ministry of health and Family, GOI, New Delhi. 1 ml of rice bran oil in 10 ml of methanol was titrated with 0.1% NaOH solution (1 gram of NaOH in 1000 ml of water) using 4 - 5 drops of phenolphthalein as end point indicator till the color changes to light pink. The reading obtained were recorded and compared against standard values.

Trans-esterification process

After obtaining the FFA content in the oil from the above process, the sample was trans esterified as per standard rules i.e. if the oil contains more than 2% FFA, the FFA is reduced first by acid catalyst esterification method (using methanol in presence of sulphuric acid) and then alkali catalyzed method [7] (using methanol in presence KOH) esterification was done. After separation of glycerol, the ester was washed to remove unreacted meth oxide. It was then heated to remove the water traces to obtain clear biodiesel. The rice bran methyl ester (biodiesel) thus obtained by this process was totally miscible with mineral diesel in any proportion. The process flow diagram for production of biodiesel is described in the Fig.2. [2-4]

Fuel properties

The fuel properties of Rice bran biodiesel and its blend were measured and tabulated in Tab. 1. Fuel properties of biodiesel and diesel were investigated for relative density at 31°C, kinematic viscosity in cSt, flash point (°C), calorific value ($\text{MJ}\cdot\text{kg}^{-1}$) and copper strip corrosion test at 50°C. The resulted fuel properties of biodiesel were compared with ASTM standards.

RESULTS AND DISCUSSION

Free fatty acids content of crude rice bran oil from titration was found to be >3.57 which was quite higher for preparation of biodiesel. Hence, Acid esterification and Alkali trans-esterification methods were followed which reduced the FFA content of Rice Bran Oil to 0.71%, which was quite low with permissible limit of 2%.

The relative density of crude rice bran oil was found to be 0.94. The values of relative density for diesel, RB biodiesel at room temperature were found to be 0.84, 0.88 respectively, while RB05 was observed to have density closer to diesel. This result confirms the findings of Mohanty (2013), who found similar results while producing biodiesel from rice bran oil [8].

The kinematic viscosity of crude rice bran oil was observed to be to be 48.4cSt at 31°C. The kinematic viscosity for diesel and RB biodiesel at room temperature were found to be 3.93 and 4.6 cSt respectively. Similar results were observed by K.C.Velappan (2007), when rice bran biodiesel and its five blends were fuelled to a CI engine [10]. The kinematic viscosity was very high for crude rice bran oil at ambient temperature but reduction in kinematic viscosity was observed after trans-esterification of the oil.

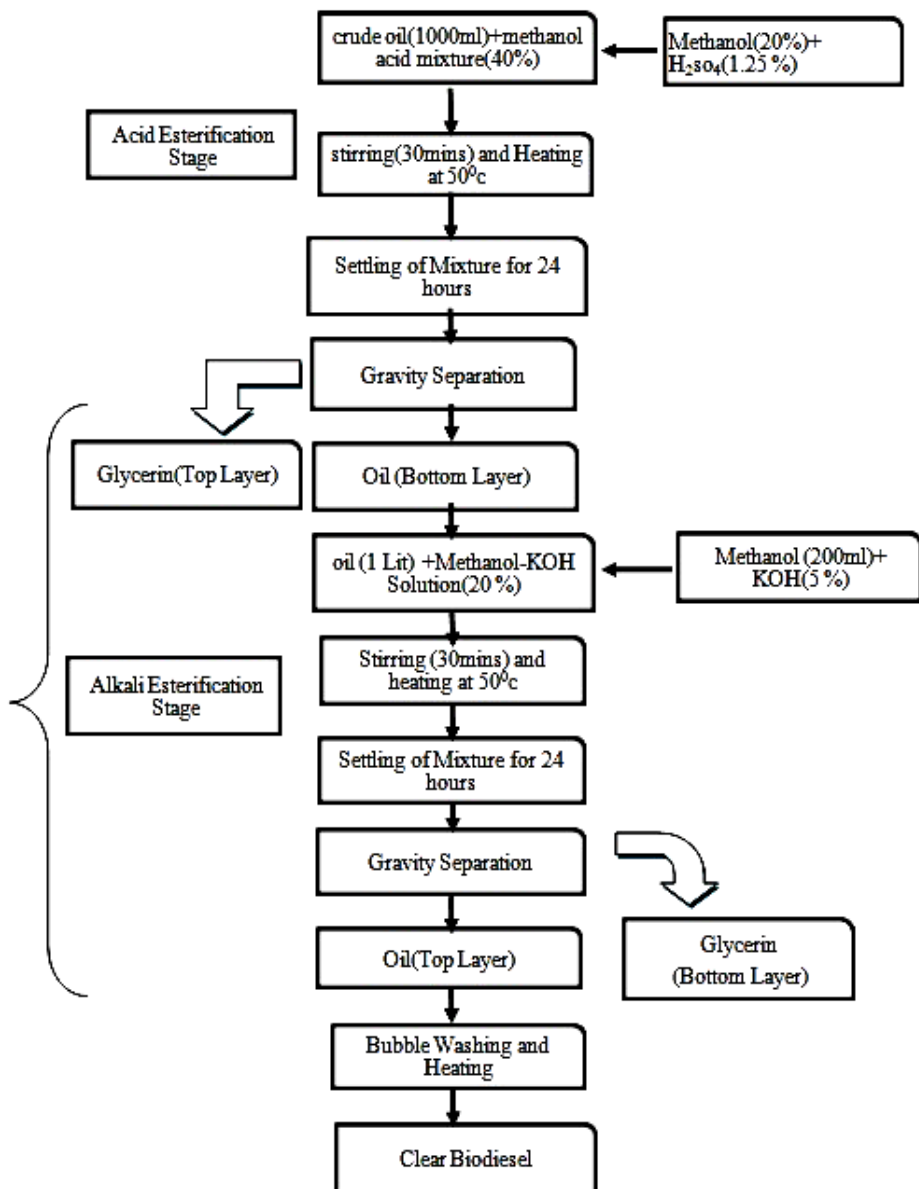


Figure 2. Process flow diagram for production of bio diesel

The calorific value for crude rice bran oil was found to be $41.36 \text{ MJ}\cdot\text{kg}^{-1}$ which is quite higher as compared to diesel. The difference in the calorific value of diesel and RB biodiesel may be attributed due to the difference in their chemical composition i.e. due to the difference in carbon and hydrogen content.

Flash point for rice bran oil was found to be 290°C, whereas trans-esterification of the oil marginally reduced the flash point temperature of the oil to 190°C. Although, higher flash point creates problem in self ignition in CI engines, but looking to the safe side of storage and handling of these biodiesels, higher flash point is more desirable.

The copper corrosion strip for evidence of tarnishing or corrosion was examined by comparing with the ASTM copper strip corrosion standards and the strip was found in transition state 1a (slight tarnish).i.e. light orange, almost same as freshly polished strip which indicates that the corrosion forming tendencies of fuel are less or equal to that of conventional diesel. Sanford *et.al.*, (2009) prepared a feedstock and reported biodiesel characteristics for different crops and found similar results. [9]

Table 1. Properties of selected fuel compared with ASTM standards

S. No.	Property	Unit	ASTM Methods	Rice bran biodiesel	Diesel
1.	Calorific value	[MJ·kg ⁻¹]	D-4809	43.171	41.382
2.	Relative density at room temperature	[g·cm ⁻³]	D-1298	0.880	0.831
3.	Kinematic viscosity at 40°C	[cSt]	D-445	4.600	3.210
4.	Flash point	[°C]	D-93	190.000	76.000
5.	Copper strip corrosion test at 50°C	-	D-130	1A (slight tarnish)	1A

CONCLUSIONS

The aim of this study was to evaluate rice bran oil as a potential raw material for biodiesel production. The biodiesel sample prepared in the present study showed better results and not deviating from ASTM standard. With the increasing demand for fuels, biodiesel can be a good substitute as it is a renewable source and can be a partial diesel substitute to boost the farm economy; reduce uncertainty of fuel availability by efficiently using it in small portable engines in rural areas for agricultural work and make fuel availability to the farmers and self-reliant. Also, this help in controlling air pollution to a great extent.

BIBLIOGRAPHY

- [1] Annonymous. 2007. *Planning Commission five year plan*. 10th Volume, Chapter 7.3.: 1-42.
- [2] Bala, B.K. 2005. Studies on biodiesels from transformation of vegetable oils for Diesel engines. *Energy Edu Sci Technology* 2005, 15: 1-43.
- [3] Debrimas, A. 2003. Biodiesel fuels from vegetable oils via catalytic and non-catalytic super critical alcohol transformation and other methods: a survey. *Energy Conversion and Management* 44; 2093-2109.
- [4] Demirbas. A. 2007. Comparison of trans-esterification methods for production of biodiesel from vegetable oils and fats. *Energy Conversion and Management* Vol. 05 (2): 1-6.

- [5] Gupta P.K., Kumar R., Panesar B.S., Thapar V.K., 2007. Parametric Studies on Bio-diesel prepared from Rice Bran Oil. *Agricultural Engineering International: the CIGRE journal*. Manuscript EE 06 007. Vol. IX. April, 2007.1-12
- [6] Kusum R. 2011. Palm oil and rice bran oil: Current status and future prospects. *International Journal of Plant Physiology and Biochemistry* Vol. 3(8): 125-132.
- [7] Maa, F., Hanna,M.A. 1999. Biodiesel production: a review. *Bioresource Technology* 70 :1-15.
- [8] Mohanty, S.K. 2013. A Production of biodiesel from rice bran oil and experimenting on small capacity diesel engine. *International Journal of Modern Engineering Research* Vol.3(2): 920-923.
- [9] Sanford, S.D. 2009. Feedstock and Biodiesel Characteristics Report. *Renewable Energy Group*, Inc., www.regfuel.com (2009): 47-86.
- [10] Velappan, K.C. 2007. Less NOx biodiesel: CI engine studies fuelled with rice bran oil biodiesel and its five blends. *Journal of scientific and industrial research* Vol. (66): 60-71.

POGODNOST ULJA PIRINČANIH MEKINJA KAO STOČNE HRANE ZA PROIZVODNU BIODIZELA

Abhinab Mishra¹, Ghanshyam Tiwari¹, Abhay Kumar Mehta¹, Sudhakar Jindal²

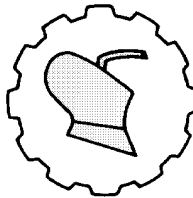
¹*Maharana Pratap Univerzitet za poljoprivredu i tehnologiju, Fakultet za tehnologiju i inžinerstvo, Institut za poljoprivredne i pogonske mašine, Udaipur, Indija*

²*Maharana Pratap Univerzitet za poljoprivredu i tehnologiju, Fakultet za tehnologiju i inžinerstvo, Institut za mašinstvo, Udaipur, Indija*

Sažetak: Indija je druga zemlja po proizvodnji pirinča, sa procenjenim prinosom ulja sirovih pirinčanih mekinja (RBO) od oko 400.000 t, od čega je samo 50% jestivo, a ostalih 50% ukupno raspoloživog ulja pirinčanih mekinja ostaje neupotrebljeno zbog prisustva aktivne lipaze u ljušci i nedostatka ekonomičnih metoda stabilizacije, pa se najveća količina ljuške koristi za stočnu hranu i industrijsku upotrebu. Jedan od najboljih načina za potencijalnu upotrebu RBO je proizvodnja biodizela; takođe, veoma malo istraživanja je izvedeno na upotrebi ovog ulja kao zamene za mineralni dizel. U ovom istraživanju biodizel je pripreman od ulja pirinčanih mekinja trans-esterifikacijom, čime je dobijen prihvatljiv kvalitet prema važećim standardima, a koji je kasnije upotrebljen kao gorivo.

Ključne reči: ulje pirinčanih mekinja, smesa, trans-esterifikacija, biodizel

Prijavljen: 18.10.2013.
Submitted:
Ispravljen:
Revised:
Prihvaćen: 07.10.2013.
Accepted:



UDK: 631.372

*Originalni naučni rad
Original scientific paper*

UTICAJ DIJAGNOSTIKE STANJA NA POUZDANOST DVOSTRUKIH POLJOPRIVREDNIH KARDANSKIH VRTAILA

Aleksandar N. Ašonja^{* 1}, Aleksandr Gennadievič Pastuhov²

¹*Srpski akademski centar, Novi Sad, Srbija*

²*Belgorodska državna poljoprivredna akademija, V.Я. Gorina, Belgorod, Rusija*

Sažetak: U radu je predstavljen model pouzdanosti dvostrukih poljoprivrednih kardanskih vratila zasnovan na dijagnostici stanja ležišnih sklopova na kardanskim zglobovima. Model pouzdanosti kardanskih vratila bio je zasnovan na ispitivanju dijagnostičkih veličinama na ležišnim sklopovima kardanskih zglobova. Osnovani cilj predloženih i izvršenih istraživanja u okviru prezentovanog rada je bila dijagnostika stanja ležišnih sklopova na zglobovima kardanskih vratila u cilju definisanja pouzdanosti kardanskih vratila. Za potrebe istraživanja isprojektovan je i izrađen laboratorijsko-optitni sto, model: "ANA", tip: modela: 23-26-26-04, koji je prvenstveno namenjen za ispitivanje pouzdanosti poljoprivrednih kardanskih vratila.

Ključne reči: pouzdanost, dvostruko kardansko vratilo, ležišni sklopovi

UVOD

Mehanizam koji je razmatran u ovom istraživanju je kardansko vratilo. Kardansko vratilo ima veliku primenu u različitim vrstama industrijskih i transportnih mašina. Elementi kardanskog vratila su opterećeni kombinovanim naprezanjem na savijanje, uvijanje, smicanje i površinski pritisak. Tokom eksploracije, usled preopterećenja, može doći do različitih vidova razaranja materijala i loma delova kardana [1].

Od četiri načina prenosa snage (mehanički, hidraulični, električni i pneumatski) od traktora do priključne mašine, u praksi najveći značaj imaju mehanički i hidraulični prenos. Za sada je mehanički prenos daleko više zastupljen od hidrauličnog. Mehanički

* Kontakt autor. E-mail: aleksandar.asonja@gmail.com

prenos snage kod poljoprivrednih mašina ostvaruje se direktno, remenicama, lančanicima, zupčanicima, kardanskim vratilima ili elastičnim vratilima [2].

Kardanska vratila danas imaju značajnu ulogu u prenošenju obrtnog momenta sa radne mašine (traktora) na priključnu mašinu. Danas, na skoro svim priključnim mašinama u poljoprivredi (prese, sejalice, rasipači mineralnog đubriva, vadilice krompira itd.) obrtni moment i snaga od traktora se uglavnom prenosi mehaničkim putem preko kardanskog vratila [3].

U eksploraciji se vek trajanja kardanskih prenosa kod poljoprivrednih mašina automobila, traktora i druge opreme koja koristi kardanske prenose, ograničava narušavanjem radne sposobnosti kardanskih zglobova u 80 - 90 % slučajeva. Sve ovo je uslovljeno nedozvoljenim povećanjem aksijalnog i radijalnog zazora i kružnog (međuigličastog) zazora u spojevima kardanskog zgloba (spoljašnjem radijalnom rukavcu vratila krstaka i igličastog ležaja) i (igličastog ležaja i otvora šoljice na viljuškama). Osnovni vidovi narušavanja pouzdanosti kardanskih prenosnika (pri uslovima pravilnog izbora veličine kardanskih vratila i isključivanja iz razmatranja pojave korozije i oštećenja površina i kvarova koji su uslovljeni grubim greškama u proizvodnji i eksploraciji) su zamor površina materijala i abrazivno habanje u 41 % i formiranje uzdužnih, često strmih, kosih udubljenja izazvanih efektom tzv. „brinevanja“ (plastična deformacija) u 45 %. Prema današnjim ispitivanjima poljoprivrednih mašina 14 % otkaza na mehaničkim prenosnicima odlazi na kardanske prenose, a na njima su oko 60 % zastupljeni otkazi kardanskih zglobova [4].



Slika 1. Primeri mogućih pojava opasnosti na dvostrukim kardanskim vratilima:

a) oštećeno vratilo na kamionu sa cisternom i b) oštećeno vratilo na poljoprivrednom traktoru

*Figure 1. Examples of the possible occurrence of hazards on a double cardan shafts:
a) the damaged shaft on a truck with tank and b) the damaged shaft on agricultural tractor*

Neki od primera snižene pouzdanosti kardanskih vratila prkazani su na Sl.1. Na Sl.1-a prikazano je oštećeno dvostruko kardansko vratilo, koje je smrtno ranilo 61-godišnjeg vozača kamiona cisterne. Nastrandali radnik je pokušao uključiti vratilo, koje je služilo za pogon pumpe na cisterni, međutim, isto je otkazalo otkačivši se na jednom od

zglobova [5]. Još jedan od primera smrte povrede koja se desila na nezaštićenom dvostrukom kardanskom vratilu u poljoprivredi u Italiji prikazan je na Sl.1-b [6].

MATERIJAL I METODE RADA

Ispitivanja pouzdanosti vršena su na dvostrukim poljoprivrednim kardanskim vratilima u laboratorijskim i eksploracionim uslovima. Za ispitivanje je korišćena veličina I dvostrukog kardanskog vratila. Korišćena je Z radna izvedba kardanskih vratila, pod uglom zakretanja 20° , Sl.2. Na Sl. 3 prikazan je ispitivan kardanski zglob u radu koji se sastoji iz 5 radnih elemenata: igličastih ležajeva, krstaka, šoljica, maziva i zaptivača.



Slika 2. Dvostruko kardansko vratilo prikazano u 3D

Figure 2. 3D image of a double cardan shaft

Slika 3. Kardanski zglob prikazan u 3D

Figure 3. 3D image of a cardan joints

Dinamičke metode ispitivanja

Od dinamičkih metoda ispitivanja pouzdanosti kardanskih vratila u radu su korišćene dinamičke metode za praćenje vibracija i temperature u kardanskim zglobovima i metoda ispitivanja broja obrtanja kardanskog prenosnika.

Dijagnostika stanja kotrlajnih ležajeva u ležišnim sklopovima je izvođena kako na zglobovima kardanskih vratila, tako i na fiksnim ležajevima pogonskog i gonjenog vratila. Na fiksnim ležajnim jedinicama, koji su bliže kardanskim zglobovima odn. koji se nalaze na kraju vratila na kojima su vezani kardanski zglobovi ispitivane su vibracije, čije vrednosti su u stvari vrednosti vibracija u ležišnim sklopovima kardanskih zglobova.

Instrumenti korišćeni za merenje bili su:

- Marlin sonda SMVL 3600 IS - za merenje nivoa vibracija,
- Laserski infracrveni termometar - za praćenje stanja temperature i
- Probator - za merenje broja obrtaja.

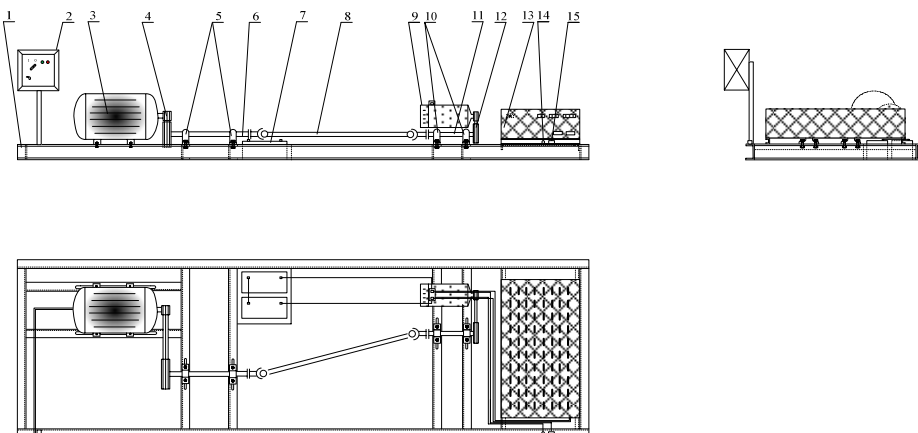
Laboratorijski sto

Za potrebe istraživanja isprojektovan je i izrađen laboratorijsko-optitni sto, model: "ANA", tip: modela: 23-26-26-04, koji je prvenstveno namenjen za ispitivanje pouzdanosti poljoprivrednih kardanskih vratila, međutim, on se može koristiti i za ispitivanje ostalih kardanskih vratila i ostalih mehaničkih prenosnika snage [7,8,9].

Osnovni delovi ovog optitnog stola, na kojem su vršena ispitivanja pouzdanosti kardanskih vratila, Sl.4, su: 1 čelična konstrukcija (postolje), 2 glavni elektro razvodni

ormar za snabdevanje strujom elektromotora i sistema za regulaciju opterećenja, 3 pogonski deo (elektromotor), 4 remeni prenosnici na pogonskom delu, 5 ležišne jedinice na prvom pomoćnom vratilu, 6 prvo pomoćno vratilo, 7 akumulatori (baterije), 8 ispitno kardansko vratilo, 9 DC generator jednosmerne struje, 10 ležišne jedinice na drugom pomoćnom vratilu, 11 drugo pomoćno vratilo, 12 remeni prenosnici na kočionom delu, 13 sistem za regulaciju opterećenja, 14 ručna regulacija pobude DC generatora i 15 kontrolna lampa pobude DC generatora [7]. Na šematskom crtežu, zbog jednostavnosti prikazivanja, izostavljen je sistem zaštite stola i sistem sa mobilnim stop tasterom.

Na laboratorijskim uzorcima kardanskih vratila ispitivana su vratila pri broju obrtanja od 540 °/min, koja su radila dok nisu dostigla ukupan broj ciklusa obrtanja od 10^7 , što odgovara dužini ispitivanja do 300 časova rada. Takođe su na laboratorijskom opitnom stolu ispitivana i poljoprivredna dvostruka kardanska vratila u predotkaznom stanju doneta iz eksploracije, na kome su merene krajne dijagnostičke veličine, kao i na uzorcima u samo laboratorijskim ispitivanjima. Za potrebe ispitivanja korišćen je promenljivi režim opterećenja po unapred određenim ciklusima od po 50 časova rada. Navedeni režimi opterećenja su režimi koji su dosta zastupljeni u praksi, radi se o potrebnoj snazi za pogon priključnih mašina (2, 3 i 4 kW) odn. 36, 55 i 75 Nm.



Slika 4. Šematski prikaz laboratorijsko-opitnog stola „ANA“ za ispitivanje pouzdanosti kardanskih vratila

Figure 4. The schematic view of the laboratory stand - "ANA" for testing the reliability of cardan shaft

Na laboratorijsko-opitnom stolu specijalno za ova istraživanja je isprojektovana i izrađena električna kočnica za simulaciju opterećenja, model: "EK", tip: 6/28. Na sistemu za regulaciju opterećenja na električnoj kočnici EK 6/28 ručno se moglo zadavati opterećenje na izlazu laboratorijskog stola, kroz vrednosti snage.

Tako se na osnovu ispisanih vrednosti (struje I i napona U) na digitalnim displejevima računala snaga P po Jed.1 odnosno vrednost obrtnog momenta M preko izmerene snage P i broja obrtaja n , Jed. 2, [7]:

$$P = U \cdot I \quad (1)$$

gde je:

P [kW] - snaga,

U [V] - napon,

I [A] - jačina struje.

$$M = \frac{P \cdot 9550}{n} \quad (2)$$

gde je:

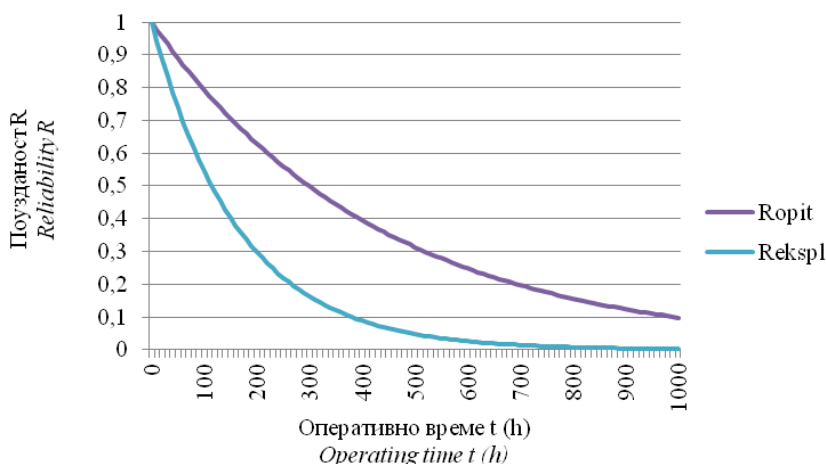
M [Nm] - obrtni moment,

P [kW] - snaga,,

n [min^{-1}] - broj obrtaja.

REZULTATI ISTRAŽIVANJA I DISKUSIJA

Na Sl. 5 prikazane su ukupne prosečne pouzdanosti posmatranih dijagnostičkih parametra temperature i aksijalnih ubrzanja vibracija na ležišnim sklopovima prvih zglobova u laboratorijskim i eksploracionim ispitivanjima. Sa Sl. 5 se može zaključiti da bi ležišni sklopovi prvih zglobova u laboratorijskim uslovima dostigli pouzdanost od 10% na ~993 h, dok bi oni u eksploracionim uslovima ispitivanja to dostigli na ~380 h.

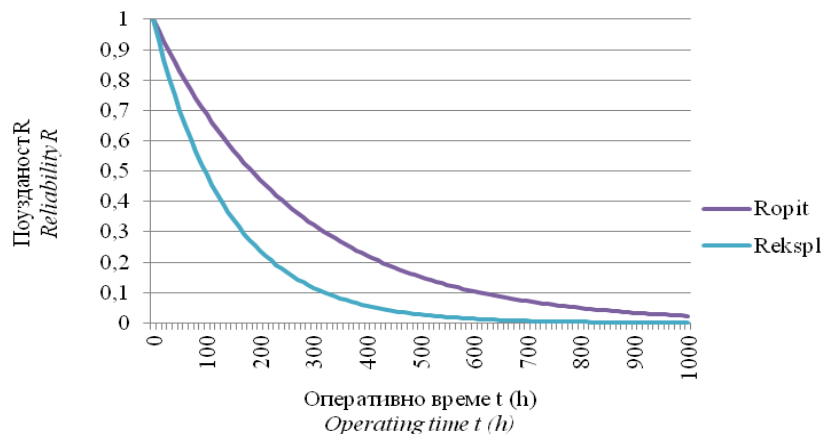


Slika 5. Ukupna pouzdanost ležišnih sklopova prvih zglobova u laboratorijskim i eksploracionim uslovima ispitivanja

Figure 5. Overall reliability of bearing assemblies of the first joints in laboratory and exploitation conditions

Na Sl. 6 prikazane su ukupne prosečne pouzdanosti za posmatrane dijagnostičke parametre temperature i aksijalnih ubrzanja vibracija na ležišnim sklopovima drugih zglobova u laboratorijskim i eksploracionim uslovima ispitivanjima. Sa Sl. 6 se može zaključiti da bi ležišni sklopovi drugih zglobova u laboratorijskim uslovima dostigli

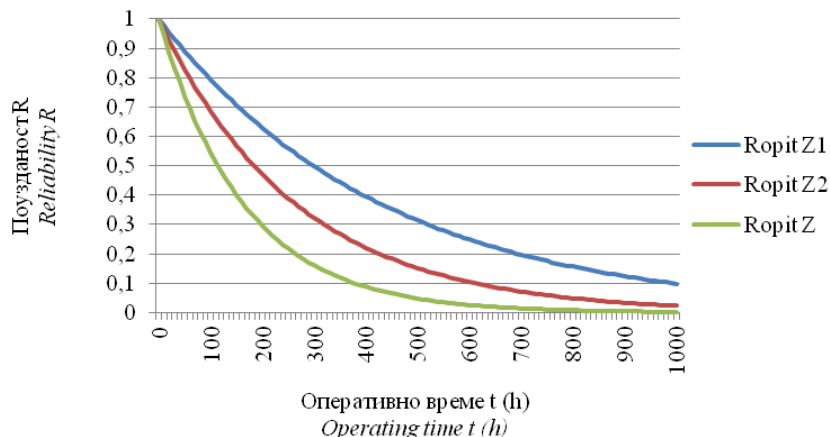
pouzdanost od 10% na ~611 h, dok bi oni u eksplotacionim uslovima ispitivanja to dostigli na ~321 h.



Slika 6. Ukupna pouzdanost ležišnih sklopova drugih zglobova u laboratorijskim i eksplotacionim uslovima ispitivanja

Figure 6. Overall reliability of bearing assemblies of the second joints in laboratory and exploitation conditions

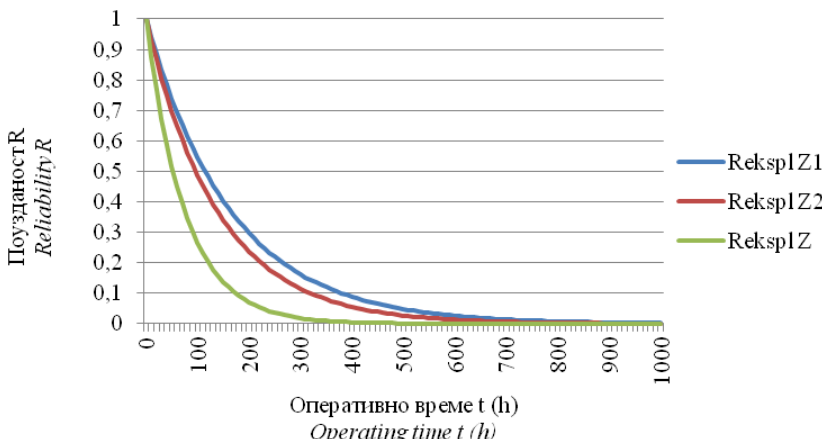
Završna ispitivanja, ukupne pouzdanosti dvostrukih poljoprivrednih kardanskih vratila, zasnovana na prosečnim pouzdanostima posmatranih dijagnostičkih parametara na prvim i drugim zglobovima za laboratorijske i eksplotacione uslove, prikazana su na Sl. 7 i 8. Na Sl. 7 vidi se da bi prosečna predviđena pouzdanost kardanskog vratila u laboratorijskim uslovima bila ~378 h rada, pouzdanost samo drugih zglobova ~611 h, dok bi prvih bila znatno viša.



Slika 7. Prosečne pouzdanosti zglobova (vratila) u laboratorijskim ispitivanjima

Figure 7. Average reliability of joints (shaft) in laboratory test

Na Sl. 8 vidi se da bi prosečna pouzdanost kardanskog vratila u eksploracionim uslovima bila ~ 174 h rada, pouzdanost samo drugih zglobova ~ 321 h, dok bi pouzdanost prvih zglobova iznosila ~ 380 h.



Slika 8. Prosečne pouzdanosti zglobova (vratila) u eksploracionim ispitivanjima
Figure 8. Average reliability of joints (shaft) in exploitation conditions

Rezultati dijagnostičkih istraživanja pri ispitivanju pouzdanosti kardanskih vratila na laboratorijskom stolu, pri uglu zakretanja vratila od 20° , ukazali su na veoma složene uslove rada. Razloge zašto se vek trajanja, dvostrukih poljoprivrednih kardanskih vratila, u eksploracionim rezultatima ispitivanja razlikuje od rezultata dobijenih u laboratorijskim uslovima i zašto je nivo eksploracije poljoprivrednih kardanskih vratila znatno složeniji, treba tražiti u sledećim konstatacijama [10]:

- nedovoljan nivo tehničkog održavanja, (prvenstveno u vršenju procesa podmazivanja koje treba da se izvodi u skladu sa preporukama proizvođača kardanskih vratila, koja su kod svih ista i izvode se na svakih 8 časova rada),
- nezaštićenost vratila od atmosferskih uticaja kako za vreme rada tako i za vreme kada se vratilo ne koristi,
- nemogućnost konstantnog održavanja paralelnih uglova na ulaznom i izlaznom vratilu, zbog veoma složenih uslova (konfiguracije terena, okretanja mašina i sl.) koji vladaju u poljoprivrednoj proizvodnji,
- nagli udari prilikom svakog uključivanja kardanskih vratila,
- promena radnih uglova u toku rada kardanskog vratila pod opterećenjem,
- prenos vibracija sa radne i priključne mašine na vibracije u ležišnim sklopovima kardanskog zgloba,
- korišćenje vratila za rad na više raznih priključnih mašina; ponekad se koriste i na mašinama čiji obrtni momenti prevazilaze ukupne dozvoljene obrtne momente na kardanskim prenosima,
- ne pridržavanje uputstava da se kardanska vratila uvek obrću u istom smeru i
- neadekvatna upotrebi.

Ključni rezultati istraživanja u okviru navedenih ispitivanja pouzdanosti dvostrukih kardanskih vratila su:

- drugi kardanski zglob na dvostrukom kardanskom vratilu je deo tehničkom sistema koji prvi otkazuje,
- veoma mala pouzdanost i vek trajanja poljoprivrednih kardanskih vratila u eksploataciji, su posledice neadekvatnog tehničkog održavanja i upotrebe, kao i složenih uslova koji vladaju u poljoprivrednoj proizvodnji,
- gotovo identične dijagnostičke parametre na praćenju ležišnih sklopova kardanskih zglobova pokazale su vrednosti aksijalnih vibracija, prvenstveno ubrzanja i temperature,
- ne preporučuje se korišćenje kardanskih vratila u eksploataciji pod uglom zakretanja $>20^\circ$, jer pri navedenim uglovima zakretanja i pri opterećenjima >75 Nm, u uslovima strogo paralelnih vratila u Z izvedbi, nivo aksijalnih vibracija (ubrzanja) ulazi u zonu nepoželjnih,
- pod uglom zakretanja dvostrukih kardanskih vratila od 20° čak i pri minimalnim korišćenim opterećenjima od 36 Nm primetno je bilo izlivanje masti iz ležišnih sklopova na oba zgloba, što je sigurno bila posledica visokog nivoa vibracija,
- pri jednosmerno promenljivim opterećenjima od 36,15, 55,25 i 74,86 Nm, dvostruka kardanska vratila u laboratorijskim uslovima ispitivanja izdržala su bez ikakvih vidljivih oštećenja do 304 h rada, dok su ona u eksploatacionim ispitivanjima izdržala u proseku 139 h rada,
- predviđena pouzdanost na dvostrukim poljoprivrednim kardanskim vratilima u eksploataciji (u trenutku vremena predotkazne pouzdanosti od 10 %), mogla bi se uvećati za $\sim 2,17$ puta i iznosila bi ~ 378 h, sl.7 i 8,
- kao najvažniji razlozi u odstupanju veka trajanja u eksploatacionim u odnosu na laboratorijska ispitivanja mogu se nabrojati: neadekvatno tehničko održavanje, složeni uslovi konfiguracije terena i eksploatacije koji vladaju u poljoprivrednoj proizvodnji, mogućnosti pojave kratkotrajnih neparalelnosti između ulaznih i izlaznih vratila i sl.,
- kao posledice nelinearnog kontakta između iglica i rukavaca krstaka odn. šoljica, na svakom rukavcu krstaka vidljiva su bila oštećenja u vidu otanjene površine na gornjem delu rukavca pod najvećim uglom od $\sim 120^\circ$, odn. na šoljicama od 100° ,
- nešto veći ugao oštećenja primetan je bio na površinama rukavaca krstaka drugih kardanskih zglobova u odnosu na prve,
- predstavljeni matematički modeli zasnovani na analizi dijagnostičkih veličina, korišćeni u analizi pouzdanosti dvostrukih poljoprivrednih kardanskih vratila, su validni i predstavljaju novinu u definisanju pouzdanosti ovakvih tipova mehaničkih prenosnika snage i
- predstavljeni matematički modeli zasnovani na analizi dijagnostičkih parametara mogu se primeniti i na ostalim mehaničkim prenosnicima snage.

ZAKLJUČAK

Analiza pouzdanosti dvostrukih poljoprivrednih kardanskih vratila koja se koriste u eksploataciji između traktora i priključne mašine, ukazuju na činjenicu da se može predvideti njihov vek trajanja. Eksploataciona ispitivanja pouzdanosti kardanskih vratila ukazala su na znatno manji vek trajanja ležišnih sklopova na kardanskim zglobovima u odnosu na sprovedena laboratorijska ispitivanja. Kao prvenstveni razlozi koji utiču na to, ističu se: neadekvatno održavanje, složeni uslovi konfiguracije terena koji vladaju u poljoprivrednoj proizvodnji, neodgovarajuća upotreba i sl.

Rezultati istraživanja pokazali su da ne treba koristiti dvostruka poljoprivredna kardanska vratila pod uglom zakretanja zglobova većim od 20° . Pod navedenim uglovima zakretanja zglobova i sa veoma malim korišćenim opterećenjima tokom ispitivanja pouzdanosti kardanskih vratila primećene su pojave veoma visokih vrednosti dijagnostičkih parametara i izlivanje maziva iz ležišnih sklopova u toku rada. Dijagnostika stanja na kotrljajnim ležajevima kardanskih vratila poljoprivrednih mašina, za date uslove korišćenja, ukazala je pre svega na sve nedostatke navedenog mehanizma u procesu eksploatacije, na osnovu kojih su predložene mere za dalje mogućnosti eksploatacije (kroz vek trajanja kotrljajnih ležajeva) u cilju povećanja pouzdanosti kardanskih vratila.

LITERATURA

- [1] Fischer, I.S., de Waal, J.K. 1995. Experimental Study of Cardan Joint Dynamics. *ASME Journal of Mechanical Design*. American Society of Mechanical Engineers, 117 (4), pp.526-531.
- [2] Ерохин, М.Н., Пастухов, А.Г. 2008. *Надежность карданных передач трансмиссий сельскохозяйственной техники в эксплуатации*. Белгородская государственная сельскохозяйственная академия, Белгород.
- [3] Ašonja, A. 2008. Ekonomска opravdanost reparacije ležišnih sklopova, *Poljoprivredna tehnika*, 33 (1), 67-73.
- [4] Пастухов, А.Г. (2008). *Повышение надежности карданных передач трансмиссий сельскохозяйственной техники*. Докторская диссертация, Белгородская государственная сельскохозяйственная академия - Московский государственный агрономический университет имени В.П. Горячкина (ФГОУ ВПО МГАУ), Москва.
- [5] Iowa FACE Program. 2002. *Tanker Truck Driver Killed by Unshielded PTO Shaft*, Case No. 2IA24, The University of Iowa.
- [6] Cecchini, M., Monarca, D., Biondi, P., Colantoni, A., Menghini, G., Brenciaglia, G. 2011. Safety of Tractor PTO Drive Shafts: Survey on Maintenance on a Sample of Farms in Central Italy. *Efficient and safe production processes in sustainable agriculture and forestry, XXXIV CIOSTA CIGR V Conference*.
- [7] Ašonja, A., Adamović, Ž., Gligorić, R., Mikić, D. 2012. Razvoj modela laboratorijskog stola za ispitivanje pouzdanosti poljoprivrednih kardanskih vratila. *Tehnička dijagnostika*, 11 (3), pp.27-32.
- [8] Ilić, B., Adamović, Ž., Jevtić, N. 2012. Automatizovana dijagnostička ispitivanja u procesnoj industriji. *Tehnička dijagnostika*, 11 (3), pp.11-18.

- [9] Ilić, B., Adamović, Ž., Jevtić, N. 2012. Primena metoda veštačke inteligencije prilikom donošenja dijagnostičkih zaključaka o stanjima mašina u procesnoj industriji. *Tehnička dijagnostika*, 11 (3), pp.33-40.
- [10] Ašonja, A., Adamović, Ž., Jevtić, N. 2013. Analysis of Reliability of Carda Shafts Based on Condition Diagnostics of Bearing Assembly in Cardan Joints. *Journal Metalurgia International*, 18 (4), pp.216-221.

THE INFLUENCE OF DIAGNOSTIC STATE OF RELIABILITY OF AGRICULTURE DOUBLE CARDAN SHAFT

Aleksandar N. Ašonja¹, Aleksandr Genadievic Pastuhov²

The Serbian Academic Center, Novi Sad

²*Belgorod State Agricultural Academy named after V. Gorin, Belgorod, Russia*

Abstract: This paper presents a reliability model of double agricultural cardan shafts based on diagnostic of the state of box-set on the cardan shaft joints. The reliability model of cardan shaft was based on an examination of diagnostic sizes of box-set on the cardan shaft joints. The main aim of the proposed and conducted research in the presented paper was diagnostic of box-set at cardan shafts joints in order to define the reliability of cardan shafts. For the needs of examination it have been designed and manufactured laboratory-examination stand, a model, "ANA", type: model: 23-26-26-04, which is primarily intended for testing the reliability of agricultural cardan shafts.

Key words: reliability, double cardan shaft, bearing assembly

Prijavljen: 12.8.2013.

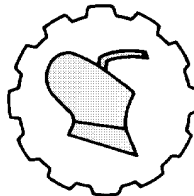
Submitted:

Ispravljen:

Revised:

Prihvaćen: 07.10.2013.

Accepted:



UDK: 621.313

*Originalni naučni rad
Original scientific paper*

COMPARISON OF THE PERFORMANCE CHARACTERISTICS OF AN INDUCTION MOTOR, THE PARAMETERS OF WHICH ARE DETERMINED EXPERIMENTALLY AND BY A GENETIC ALGORITHM

Anka Krasteva^{*}, Donka Ivanova, Miglena Hristova

*University of Ruse, Faculty of Electrical and Electronic Engineering and Automation,
Ruse, Bulgaria*

Abstract: In the present study, the parameters of the T-shaped equivalent circuit of an induction motor (IM) are defined by way of experiment and by using a genetic algorithm. An algorithm is constructed for obtaining data about the performance characteristics of an IM through models created in the Matlab/Simulink environment. A virtual setup is developed by means of which a comparison is made of the performance characteristics of an IM, the parameters of which are obtained experimentally and by a genetic algorithm. The relative errors for the studied values are determined and reasonable grounds are given for the possibility of using a genetic algorithm to determine the parameters of the equivalent circuit.

Key words: *induction motor, Matlab/Simulink, genetic algorithm*

INTRODUCTION

In order to compute the performance and mechanical characteristics of induction motors and determine their efficiency at different loads, the exact values of the parameters (resistance and inductive reactance of the stator and rotor windings and of the magnetizing circuit) from the equivalent circuit of an induction motor (IM) have to be known.

^{*} Corresponding author. E-mail: akrasteva@uni-ruse.bg

For determining the equivalent circuit parameters of IM, a number of methods have been created and new ones are continuously being developed. Most generally, these methods can be classified in two groups: analytical and experimental.

The analytical methods, according to the data that are used for determining the equivalent circuit parameters, are as follows: method based on the motor nameplate data; method of catalog data; method of reference data; etc.

The classic experimental method is based on data from the no-load test and short-circuit test and is difficult to apply in practice but the parameters defined through it correspond with high accuracy to the specific motor being tested. New contemporary experimental methods for determining the parameters of IM have been developed that allow avoiding the carrying out of no-load and short-circuit tests. In some, a genetic algorithm is used [1, 2], which optimizes the data from measurements at different loads of the supply voltage, current, power consumption, stator winding resistance, and rotational speed, in order to obtain the parameters of the T-shaped equivalent circuit.

The purpose of this study is by means of a virtual setup to take and compare the data necessary to build the performance characteristics of an induction motor (IM), with the parameters of the T-shaped equivalent circuit being determined by two different methods – experimentally and by using a Genetic Algorithm (GA).

MATERIAL AND METHODS

A block diagram is given in Fig. 1, in which the steps for obtaining data about the performance characteristics of an IM by means of a virtual setup are specified. The IM parameters are determined by two different methods – experimentally, and by using a Genetic Algorithm (GA). During the first step, experiments have been held in laboratory conditions with an induction motor (IM) of the type 1LA9083-2KA60, energy efficiency class EEF1, with the following catalogue data: Rated power $P_r = 1,1 \text{ kW}$, rotational speed $n_r = 2860 \text{ min}^{-1}$, rated voltage $U_r = 400V$, rated current $I_{lr} = 2,1A$, efficiency $\eta = 0,85$, power factor $\cos \varphi = 0,89$, delta connection of the stator winding. To compute the parameters of the T-shaped circuit (Fig. 2) of the IM based on experimental data, the methodology described in [3] is applied.

The necessary input data according to the methodology are as follows: rated nameplate data of the IM, stator winding resistance, no-load and short-circuit test results. The no-load test provides the measured values for the current I_o , voltage U_o and power P_o at rated voltage, and the short-circuit test provides the current I_k , voltage U_k and power P_k at rated current.

The stator winding resistance R_l is measured using a measuring bridge or by the ammeter and voltmeter method with DC supply.

Based on the data obtained in the experimental study of the IM, the values of resistance and inductive reactance of the stator winding $R_l = 13,16\Omega$, $X_l = 18,05\Omega$, and rotor winding $R_2' = 20,03\Omega$, $X_2' = 18,05\Omega$ and of the magnetizing circuit $X_\mu = 799,31 \Omega$ have been measured by the methodology, described in [3].

In order to determine the parameters of the T-shaped equivalent circuit of the IM using a GA (second step in Fig.1) the objective function is necessary to be selected, by means of which to obtain results similar to the ones produced experimentally.

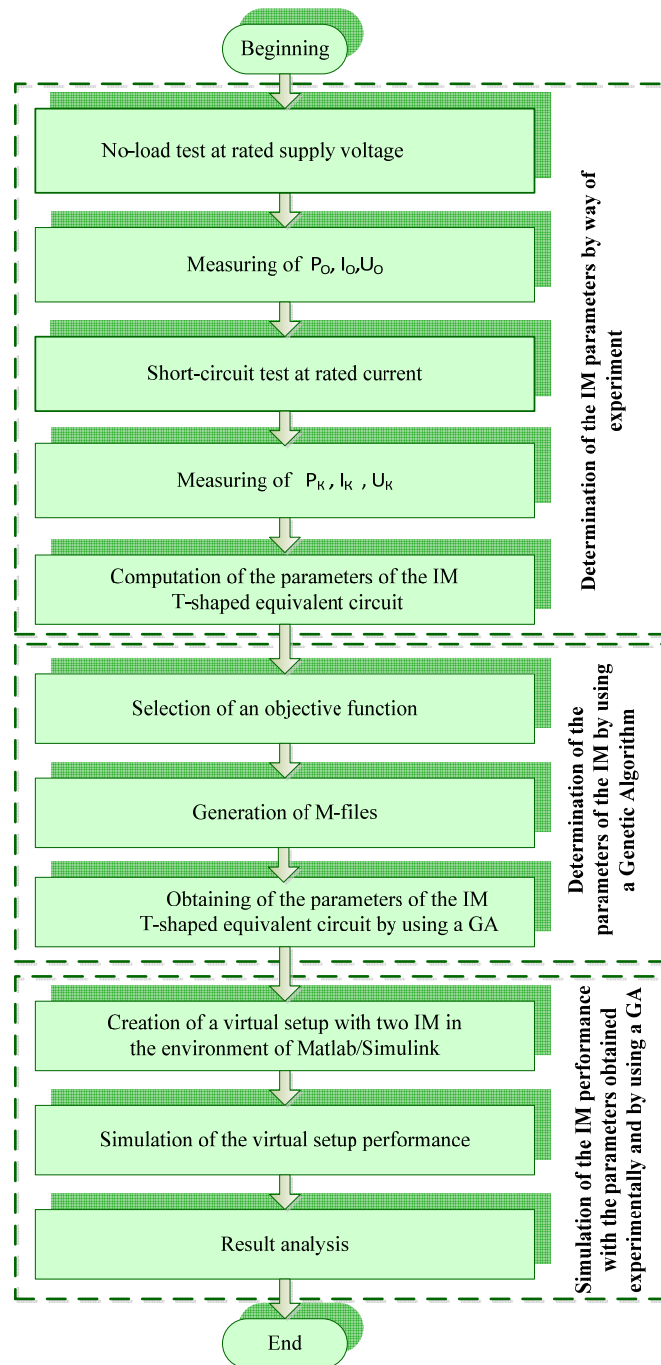


Figure 1. Algorithm for obtaining data on the IM performance characteristics using models in the Matlab/Simulink software environment

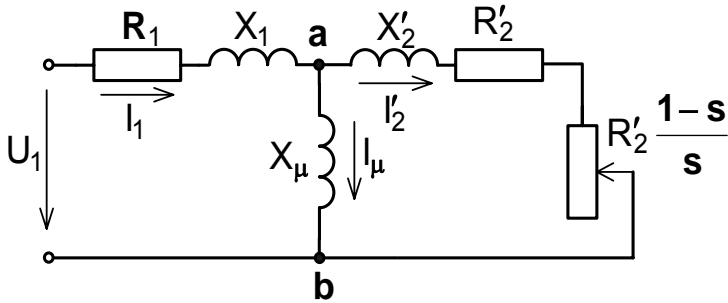


Figure 2. T-shaped equivalent circuit of an IM

RESULTS AND DISCUSSION

To create the objective function, it is necessary to define the equivalent resistance R_{eq} , the equivalent inductive reactance X_{eq} and the impedance Z_{eq} of the equivalent circuit using the following formulas:

$$R_{eq} = R_I + \frac{\frac{X_\mu^2 R'_2}{s}}{\left(\frac{R'_2}{s}\right)^2 + (X'_2 + X_\mu)^2}; \quad (1)$$

$$X_{eq} = X_I + \frac{\left(\frac{R'_2}{s}\right)^2 X_\mu + X'_2 X_\mu (X'_2 + X_\mu)}{\left(\frac{R'_2}{s}\right)^2 + (X'_2 + X_\mu)^2}; \quad (2)$$

$$Z_{eq} = \sqrt{R_{eq}^2 + X_{eq}^2}. \quad (3)$$

In the M-file of the GA, the power factor $\cos \varphi$, current consumption I_l , power consumption P_l are computed by the formulas:

$$I_l = \frac{U_l}{Z_{eq}}; \quad (4)$$

$$\cos \varphi = \cos \left(\arctan g \frac{X_{eq}}{R_{eq}} \right); \quad (5)$$

$$P_l = 3U_l I_l \cos \varphi. \quad (6)$$

For the study, the following objective function is selected, where n is the number of data groups:

$$F = \sum_{i=1}^n \left(\frac{\cos \varphi_{ie}}{\cos \varphi_{im}} - 1 \right)^2 + \sum_{i=1}^n \left(\frac{I_{lie}}{I_{lim}} - 1 \right)^2 + \sum_{i=1}^n \left(\frac{P_{lie}}{P_{lim}} - 1 \right)^2 \quad (7)$$

The measured values are marked with an index „e“, while the values computed through *GA* have an index “m”. The experimentally obtained data for I_{ie} , $\cos \varphi_{ie}$, P_{ie} and slip serve as input data to the *GA*. To determine the objective function optimum value (7), I_{im} , $\cos \varphi_{im}$ and P_{im} are computed from the equations (4), (5) and (6). Output data of the *GA* are the parameters of the *T*-shaped equivalent circuit.

This paper presents the solution of the optimization problem by a *GA* using two sets of experimental data. They are obtained from the study of an IM in laboratory condition for two different loads (P_2/P_{2r}) – 28,18% and 93,80%. The IM is loaded by a separately excited DC generator. The resulting values for the phase voltage U_I , current I_I , power consumption P_I , rotational speed n , power factor $\cos \varphi$, motor shaft effective power P_2 are given in Tab. 1.

Table 1. Experimental results from the load test of an IM of EEEI energy class

U_I [V]	I_I [A]	P_I [W]	n [min ⁻¹]	P_2 [W]	$\cos \varphi$ [-]	P_2/P_{2r} [%]
391	0,570	374,1	2960	310,00	0,559	28,18
391	1,215	1266,0	2846	1031,85	0,887	93,80

For solving the optimization problem, limitations are set on the equivalent circuit parameters. The range is specified within which their values change in relative units [4].

An M-file is generated that includes the object function, the experimental data from Tab. 1, and the basic dependencies (1) to (7) determined according to the circuit in Fig. 2. The solution of the optimization problem using a Genetic Algorithm produces the following values for the resistance and inductive reactance of the stator winding: $R_l = 15,99 \Omega$, $X_l = 16,56 \Omega$ and rotor winding: $R'_l = 18,44 \Omega$, $X'_l = 16,56 \Omega$ and for the magnetizing circuit $X_\mu = 775,59 \Omega$.

At the third step of the algorithm described in Fig. 1, a virtual setup (Fig. 3) is created, with two *IM*, *AD1* and *AD2*, and the performance of the setup at different loads is simulated. The parameters of the equivalent circuit of *AD1* are determined experimentally, while those of *AD2* – by a *GA*. The proposed setup is used to compare the performance characteristics of the two motors.

For the designing of the stand, two completed blocks of a three-phase induction machine, designated as *AD1* and *AD2*, are used. The motors are powered by a Three-Phase Programmable Voltage Source. At the output of the Machines Measurement Demux1 and Machines Measurement Demux2 blocks information is obtained about the currents in the stator winding in different coordinate systems, the angular speed, electromagnetic torque, other state variables, which are fed to the input of the developed Performance 1 and Performance 2 subsystems. They are used to obtain data about the current consumption I_I , power consumption P_I , power factor $\cos \varphi$, rotational speed n , efficiency, motor shaft torque M_2 , motor shaft effective power P_2 that are necessary to construct the performance characteristics of the induction motor.

The data about the performance characteristics of an IM, the parameters of which are determined experimentally and by a *GA*, are compared using the relative error δ . Its percentage value is computed by the developed subsystem Relative error that has 14

inputs and 3 outputs. The relative error δ of the studied values is computed by the formula:

$$\delta = \left| \frac{x_2 - x_1}{x_1} \right| 100, \%, \quad (8)$$

where X_1 is the value obtained from simulation on the virtual setup for $AD1$, while X_2 is the value obtained for $AD2$.

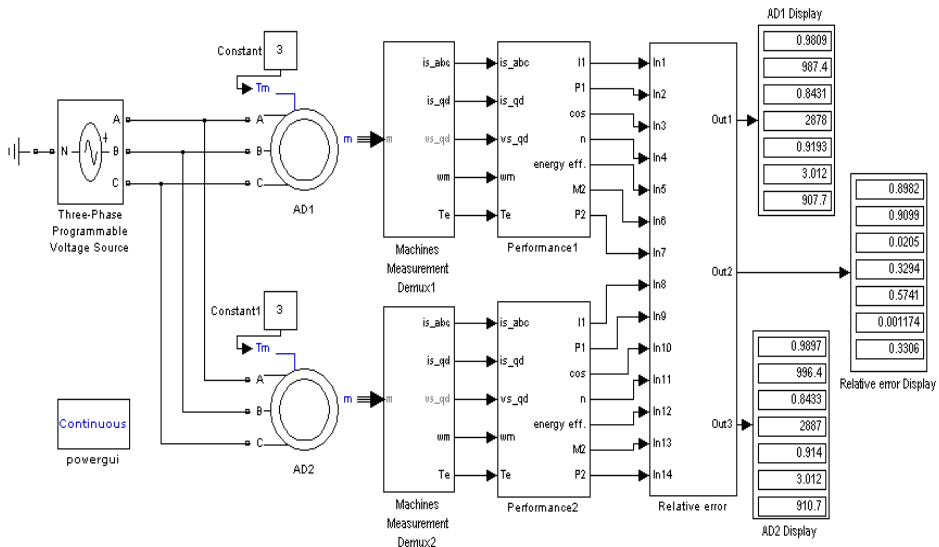


Figure 3. Virtual setup for taking the performance characteristics of an induction motor in the Matlab/Simulink environment

Table 2 Data about the relative error obtained for the two IM for which the parameters are determined experimentally and by using a GA at different relative loads (RL)

RL	δ_I	δ_{P_I}	$\delta_{\cos\varphi}$	δ_n	δ_η	δ_{M_2}	δ_{P_2}
%	%	%	%	%	%	%	%
10	3,028	2,290	0,693	0,041	2,126	0,074	0,115
25	2,387	1,086	1,244	0,103	0,956	0,017	0,111
50	1,451	0,845	0,564	0,204	0,610	0,025	0,229
75	0,970	0,906	0,563	0,301	0,566	0,033	0,335
100	0,809	1,017	0,205	0,400	0,615	0,005	0,395

To the first seven inputs of Relative error information is supplied for the values of the performance characteristics of the first motor, and to the inputs from 8 to 14 -of the second one, respectively. The display connected to output 1 visualizes the values for $AD1$, and the one connected to output 3 is used for $AD2$. From output 2 information is received for the relative error.

The procedure for adjustment of the individual blocks in the circuit is described in detail in [5, 6].

Table 2 shows the relative error δ of the studied values for the IM the parameters of which are determined experimentally and by a *GA*.

The highest relative error - 3.028% in the study is received for the current consumption at a relative load of 10%. From Tab. 2 it is evident that the errors for the other tested values are very small. On these grounds it can be asserted that by using a *GA* to determine the T-shaped equivalent circuit parameters of an IM, and the suggested virtual setup, we can receive data about the performance characteristics of an IM which describe with sufficient accuracy the data about the performance characteristics obtained by the simulated operation of an *IM* the parameters of which are determined by way of experiment.

CONCLUSIONS

An algorithm has been drawn up for obtaining data based on which the performance characteristics of an *IM* can be built in the Matlab/Simulink environment.

With the use of data about two different loads applied to a *VFD* and a *GA*, the parameters of the T-shaped equivalent circuit are determined. A virtual setup is created, in which the performance of an *IM* is simulated after obtaining the parameters of its T-shaped equivalent circuit in two different ways – experimentally, and by using a Genetic Algorithm. The obtained values for the relative errors of the studied parameters are very small, up to 3%. Therefore, the Genetic Algorithm can be used to determine the parameters of the equivalent circuit with sufficient accuracy, without carrying out no-load or short-circuit tests. Thus it is possible to easily take the performance characteristics of an induction motor by means of a virtual setup and to determine the power indices of automated drives at different loads.

BIBLIOGRAPHY

- [1] Ertan, B., Leblebicioglu, K., Avenoglu, B., Ercan, B. 2003. Identification of parameters of an induction motor from field solution. *Proceedings of the Sixth International Conference on Electrical Machines and Systems ICEMS 2003*, Vol. 1, 2003 , pp. 1-6.
- [2] Kostov, I., Spasov, V., Rangelova, V. 2009. Application of genetic algorithms for determining the parameters of induction motors. *Scientific-professional journal of technical faculties of the University of Osijek*, 2009, Vol.16, pp. 49-53.
- [3] Христова, М. 2011. Методика за определяне на товарването и коефициента на полезно действие на асинхронните двигатели. *Енергетика*, 2011, брой 4, стр. 25-29.
- [4] Волдек, А. 1971. *Електрически машини*. ДИ Техника. София. 1971.
- [5] Христова, М., Кръстева, А. 2012. Изследване на трифазен асинхронен двигател в програмната среда на Matlab/Simulink. *Известия на съюза на учениците*. Русе, 2012.
- [6] Черных, И.В. 2008. *Моделирование электротехнических устройств в MATLAB, SimPowerSystems и Simulink*. М. ДМК Пресс, Москва 2008.

**POREĐENJE KARAKTERISTIKA JEDNOG INDUKCIONOG MOTORA,
ČIJI PARAMETRI SU ODREĐENI
EKSPERIMENTALNO I GENETIČKIM ALGORITMOM**

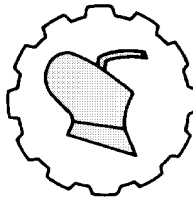
Anka Krasteva, Donka Ivanova, Miglena Hristova

*Univerzitet Ruse, Fakultet za elektrotehniku, elektroniku i automatizaciju,
Ruse, Bugarska*

Sažetak: U predstavljenom istraživanju, parametri T-ekvivalentnog kola jednog indukcionog motora (*IM*) su definisani eksperimentalno i upotrebom genetičkog algoritma. Algoritam je formiran za dobijanje podataka o performansama jednog *IM* kroz modele koji su kreirani u Matlab/Simulink okruženju. Virtuelni setap je razvijen poređenjem karakteristika jednog *IM*, čiji parametri su određeni eksperimentalno i genetičkim algoritmom. Za proučavane vrednosti su određene relativne greške i date su logične osnove za mogućnost upotrebe genetičkog algoritma za određivanje parametara ekvivalentnog kola.

Ključne reči: *indukcioni motor, Matlab/Simulink, genetički algoritam*

Prijavljen: 04.10.2013
Submitted:
Ispravljen:
Revised:
Prihvaćen: 12.01.2014.
Accepted:



UDK:621.31

*Originalni naučni rad
Original scientific paper*

RESULTS FROM A STUDY ON THE TEMPERATURE OF SOLAR MODULES

Konstantin Koev*, Krasimir Martev

University of Ruse “Angel Kanchev”, Faculty of Electrical and Electronic Engineering and Automation, Department of Electrical Power Engineering, Ruse, Bulgaria

Abstract: A research was made on the influence of the temperature of stationary photovoltaic modules on the production of electricity. The modules are connected in groups, with a total maximum installed capacity of 117.24 kWp. They are mounted on the roof of a non-residential building, located in an uninhabited area. The study covers several typical months in the period from January 2009 to December 2012. The produced electricity changes in the interval 0 - 25.55 kWh, for a temperature difference between the photovoltaic modules and the environment in the range of -5 to +30° C.

Key words: photovoltaic modules, temperature of the modules, electrical energy, overheating, cooling

INTRODUCTION

One method of converting the energy of the solar radiation is through the use of the photovoltaic effect [1]. It is used widely in the photovoltaic cells and panels for receiving electrical power. The biggest advantages of this technology are the availability of virtually unlimited amounts of free energy source (solar radiation) and the lack of hazardous waste [2]. Major disadvantage of the photovoltaic modules is their low efficiency (efficiency), the values of which decreases continuously during operation [3].

Several studies show that the characteristics of the photovoltaic modules depend on their temperature [4]. Therefore are proposed models of these relationships through which are examined and predicted the duration and effectiveness of the operation of photovoltaic modules [5].

* Corresponding author. E-mail: kkoev@uni-ruse.bg

The purpose of this study is to analyse the changes in the power output, related to the overheating of photovoltaic modules in the region of Rousse, Bulgaria.

MATERIAL AND METHODS

Subject of the study

The examined object is a photovoltaic system with a total maximum power of the modules 117.24 kWp [6]. The modules are located on the roof of a non-residential building, located in an uninhabited territory at an altitude of 76 m and in a moderate continental climate. The site is located in the region of Ruse, near the Danube river.

The chosen site is unique for several reasons. The photovoltaic system is with power more than 100 kWp and is built on a roof structure. The area of the city of Ruse, where the system is established is characterized by the second largest in Bulgaria annual average intensity of solar energy $1450 - 1500 \text{ kWh} \cdot \text{m}^{-2}$ [7]. Another feature of the object is that it is composed of more than one type of photovoltaic modules, arranged in rows and sections. This is a prerequisite for making comparative analysis of the climate characteristics of the modules by types, sections and rows.

The total number of the modules is 824, and 528 of them have a maximum power - 130 Wp. They are arranged in 4 lines, with 3 sections (Fig. 1) and in each section are mounted 44 modules. The remaining 324 modules have a maximum power of 150 Wp each, and are located in the northern part of the roof (Fig. 1). These modules are divided into 6 sections, each comprising 54 modules, arranged in 2 rows.

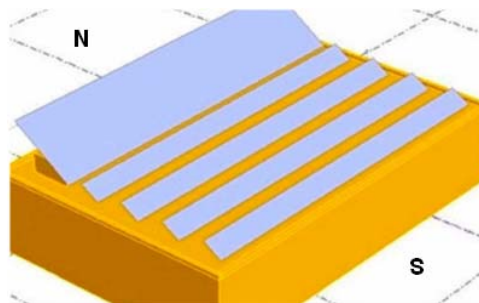


Figure 1. Location of the modules in sections and rows on the roof: N - north; S - south

The produced electrical energy is converted by inverters fitted to each section of photovoltaic modules. The total number of inverters is 18.

Methods and tools for the study

Solar irradiation and the temperature of the modules are the main factors determining the production of electricity from photovoltaic modules [1,3]. The first factor is decisive, because it also affects the temperature of the modules.

The electricity output is determined by the information received from the inverters, and recorded every 15 minutes.

The temperature of the modules and the environment is measured by a resistive transducers type Pt100, with range -40 to $+125^{\circ}\text{C}$ and accuracy of $\pm 0,5^{\circ}\text{C}$. The values of the temperatures recorded at the same interval as the electrical energy - 15 minutes.

Very often, rather than the temperature of the photovoltaic modules, it is convenient to monitor the temperature of their overheating compared to the ambient temperature [8]. It is represented as the difference between the temperatures of the modules T_m and the environment T_a , i.e. $(T_m - T_a)$. Overheating temperature gives an idea of the thermal regime in which the modules operate at different ambient temperatures. This is particularly important in photovoltaic modules, because they are made of semiconductor cells, for which the parameters strongly depend on the temperature [1,3].

RESULTS AND DISCUSSION

In the study are examined four years from the operation of photovoltaic modules - 2009 - 2012, in the specific geographic conditions. Processed data cover the months during which are produced the greatest amounts of electricity for the year. These months are May of 2009, August of 2010, and July of 2011 and 2012.

Produced quantities of electric energy E from the photovoltaic plant are different for each month throughout the year and the decisive point is the influence of solar irradiation. Its power intensity set for 1 m^2 area of photovoltaic panels is amended periodically. The maximum values of the intensity are observed during the summer months, and the minimum - in the winter. This is explained by the latitude at which the object is located.

Electricity output for the period 2009 - 2012 is presented in Fig. 2. Below are the total electrical energy per year (kWh) and the months with the highest production during the year (% of annual production). Comparing the values for the entire period shows that the amount of electricity produced is highest in July 2012 - 19 707.25 kWh. This year the production is also the largest - 154 315.8 kWh, as in July were generated 12.77% of this amount.

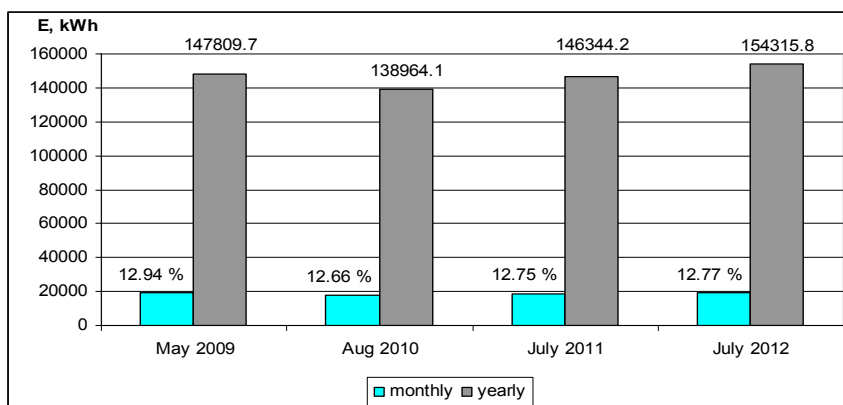


Figure 2. Generated electricity for the period 2009 - 2012 by year and month with the highest production in the respective year

The analysis of the data indicates that the total amount of electricity produced in 2009, is higher than that in 2011 by 1 465.5 kWh. This is 1% of the quantity produced during 2011. In addition, the share of the month with the highest production for 2009 - May is the highest for the four years - 12.94% (Fig. 2). For these reasons, the data for 2009 are an exception from the trend for changes of production in the period 2010 - 2012. Then there is an increase in both the total annual quantity of electricity, and the share of the month with the highest production. The generated electricity in May 2009 was 19119.34 kWh, and in July 2012 was 19707.25 kWh. The share of these amounts in the total annual production is respectively 12.94% and 12.77%. The difference in the final values is due to the fact that the total annual electricity production in 2009 was lower than in 2012.

The observed changes in electricity production are mainly due to the changes in weather conditions under which works the photovoltaic system. These changes affect the performance of the modules, as the main factor is the thermal regime. It is determined by the solar irradiation and the conditions of cooling. This requires to be studied the influence of the temperature of the modules on the production of electricity.

Collected and processed are data for the production of electricity for the months considered - May 2009, August 2010, July 2011 and 2012. The amounts of energy and module temperature T_m and the environment T_a are recorded every 15 min. PV modules generate electricity only during daylight when solar irradiation is large enough. In some clear nights, especially on a full moon, are registered very small amounts of energy produced (several tens Wh). This is due to the limited light flux of the moon. For these reasons, the data for the energy and temperature are presented and analyzed only for the hours of daylight.

In Fig. 3 - Fig. 6 are presented the dependencies of the produced electrical energy E , kWh, the difference in temperature ($T_m - T_a$), °C, for the four months considered, for each day of the month.

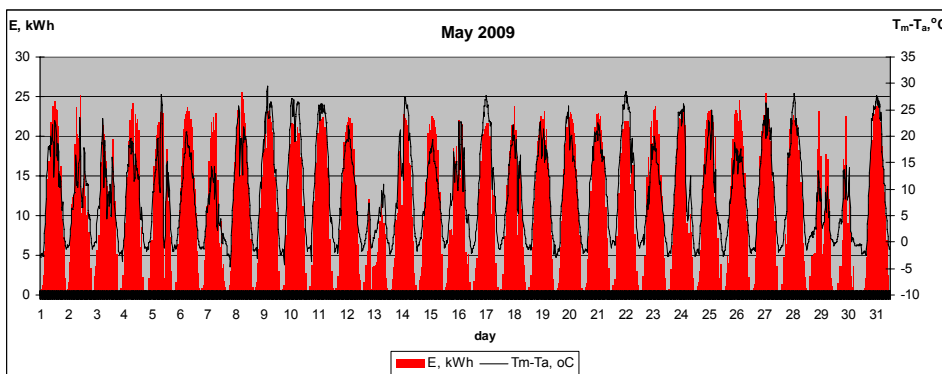


Figure 3. Changes of the produced electrical energy E , kWh, depending on overheating ($T_m - T_a$), °C, for each day of May 2009

The comparison of the graphs (Fig. 3, 4, 5 and 6) for the impact of the difference in temperature ($T_m - T_a$) (overheating modules) on electricity produced E , for each day of the month makes it possible to be detected some particularities. Every day of the four

months is characterized by a bell rescheduling of the energy produced. There are exceptions, which are least in July, 2012. The charts of the electricity produced are in accordance with the daily changes of solar irradiation [9], which is explained by the strong influence of the latter [10].

The maximum values of the electricity produced in the four months are registered during the midday hours and fluctuate between 20 - 25.55 kWh. It can also be noticed some exceptions - 13th day of May, 2009, 5th, 16th, 30th and 31st of August, 2010, the 3rd of July 2011 and 30th of July 2012. The considerably small and irregular performance of the photovoltaic system in these days is due to the dynamic changes in solar radiation. The latter are due to frequent changes in the cloud cover.

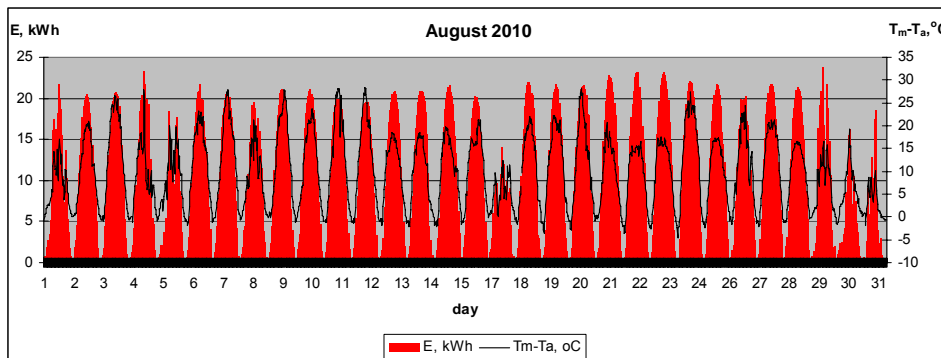


Figure 4. Changes of the produced electrical energy E , kWh, depending on overheating ($T_m - T_a$), °C, for each day of August, 2010

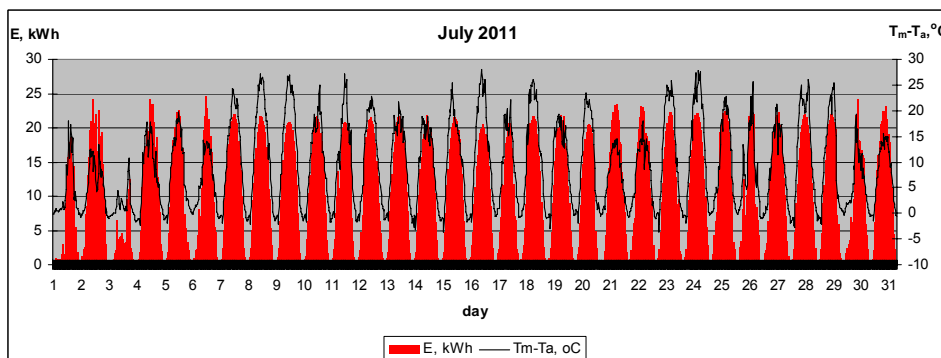


Figure 5. Changes of the produced electrical energy E , kWh, depending on overheating ($T_m - T_a$), °C, for each day of July, 2011

The graphs (Fig. 3, 4, 5 and 6) impede the analysis of the functional relationship between the studied variables - temperature of the overheating ($T_m - T_a$) of photovoltaic modules and their electricity output E . The analysis shows that it is more appropriate to present the changes of the energy output only depending on the temperature of overheating, without showing the changes in the individual days (Fig. 7, 8, 9 and 10).

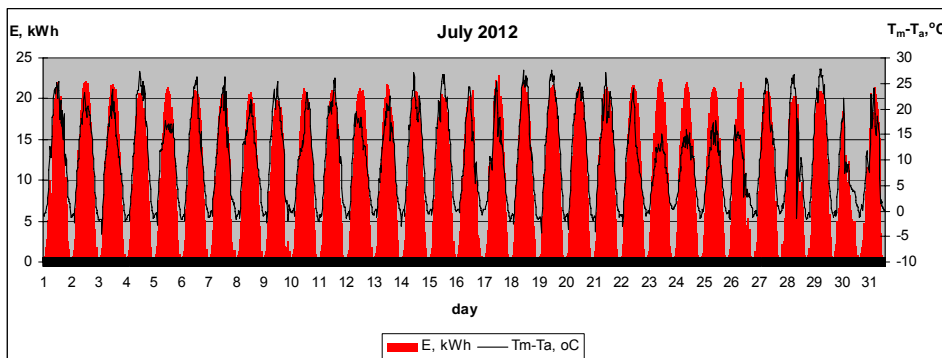


Figure 6. Changes of the produced electrical energy E , kWh, depending on overheating ($T_m - T_a$), °C, for each day of July, 2012

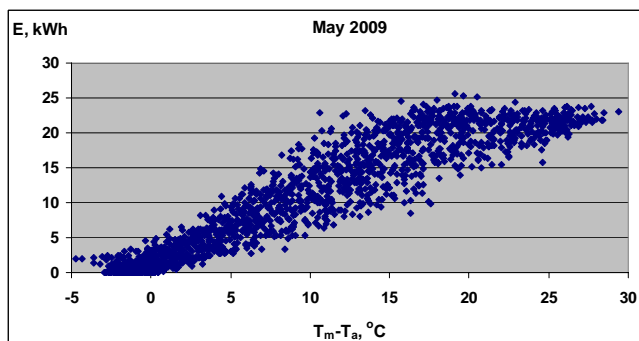


Figure 7. Effect of overheating ($T_m - T_a$) of photovoltaic modules on their electricity output E , in May 2009

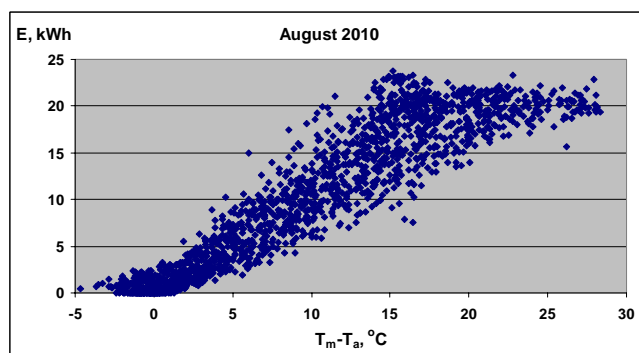


Figure 8. Effect of overheating ($T_m - T_a$) of photovoltaic modules on their electricity output E , in the month of August 2010

When comparing the graphical dependence $E = f(T_m - T_a)$ for the four months considered, can be seen that they have approximately the same nature of change. The

values of the electrical power are positive, increasing from 0 and reaching 22 - 25 kWh. Only in May 2009, are reported several values above 25 kWh, the maximum of which is 25.55 kWh. These features can be explained by the relatively high solar radiation and better cooling conditions, in comparison with typical summer months.

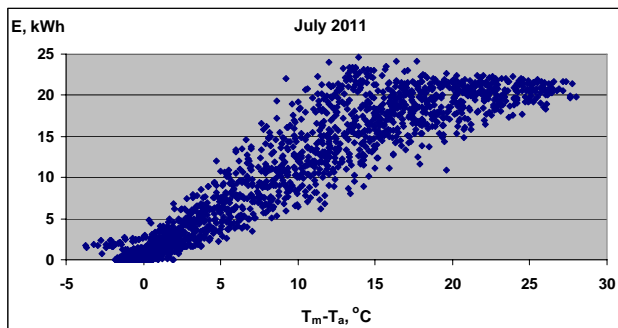


Figure 9. Effect of overheating ($T_m - T_a$) of photovoltaic modules on their electricity output E , in July 2011

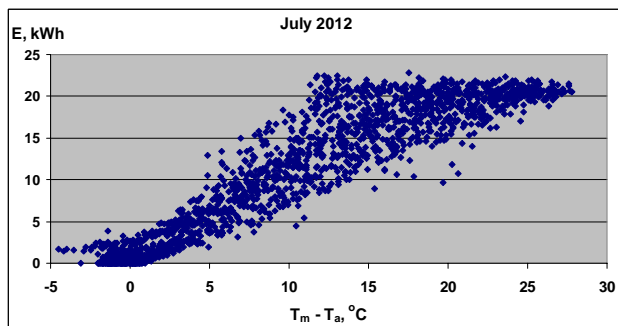


Figure 10. Effect of overheating ($T_m - T_a$) of photovoltaic modules on their electricity output E , in the month of July 2012

From the graphs can be observed the presence of "threshold" value of the temperature of overheated modules ($T_m - T_a$), above which the maximum electrical energy output is increasing. This limit is different for the different months and approximately is 17°C in May 2009 (Fig. 7), 15°C in August 2010 (Fig. 8) and July 2011 (Fig. 9) and 13°C in July 2012 (Fig. 10). Therefore, the greatest threshold value of overheating modules was observed in May 2009. The probable cause for this is the better cooling. It can be assumed that the changes in the latter, cause a larger scatter of the values of the produced energy E , when there is overheating of PV modules in the interval $(T_m - T_a) = 5 - 20^\circ\text{C}$ (Fig. 7, 8, 9 and 10).

On all the graphs (Fig. 7, 8, 9 and 10) can be seen that the values of the electric energy produced E is characterized by variable diffusion and ambiguity. The latter is expressed in the fact that a particular value of the energy E correspond to several values

of modules overheating ($T_m - T_a$). The reason for this ambiguity may be explained by the differing conditions of the cooling of the photovoltaic modules.

Overheating of the modules ($T_m - T_a$) for all the months is characterized by small negative values. They are in the range -5 to 0°C and are in accordance with the electrical energy produced $E = 0 - 5$ kWh. Negative values of overheating are observed at the start and in some cases at the end of days. At the beginning of Day $T_m < T_a$, because the modules are cooled during the night and time passes while they are heated to or above the ambient temperature T_a . At the end of the day the modules are cooling and their temperature T_m decreased, and in most cases it is close in value to the ambient temperature T_a , but it does not fall below it. Therefore, overheating of the module ($T_m - T_a$) in the evening hours is in the range 0 - 1°C. In some days, with better cooling (e.g., wind), the modules cool down more rapidly than the surrounding air. Then $T_m < T_a$ and are recorded negative values of the overheating ($T_m - T_a$).

CONCLUSIONS

Collected and processed are data for the operation of a photovoltaic system with a total maximum power 177.24 kWp, located near the town of Ruse. Analysed are the data for the months with the highest annual quantity of electricity produced in the period 2009 - 2012. The study addresses the influence of the temperature of the PV modules T_m on the production of electricity E by the temperature of overheating ($T_m - T_a$).

It was found that the functional dependencies $E = f(T_m - T_a)$, for all the months were similar, but ambiguous. This is due to the variety of operating conditions - the solar irradiation and thermal regime (cooling). It can be assumed that the ambiguity will be eliminated if the analyses are performed at unchanging solar radiation.

The values of electrical energy E vary in the range (0 - 25.55) kWh, rising continuously until they reach a maximum "threshold" value. The latter changes in the interval 13 - 17°C.

The temperature of overheating of the modules ($T_m - T_a$) changes in the interval -5 to + 30°C. The negative values -5 to 0°C, are due to changes in the conditions of cooling of the modules - the temperature of the modules T_m is less than the ambient temperature T_a , in the morning hours of the days and in some cases - in their evening hours.

Complete picture of the influence of the temperature of overheating of the modules ($T_m - T_a$) on electricity produced from photovoltaic modules E can be obtained by an investigation for more months. It is then possible to model the functional relationship $E = f(T_m - T_a)$ even at various values of the solar irradiation.

BIBLIOGRAPHY

- [1] 2008. *Planning and installing photovoltaic systems : a guide for installers, architects, and engineers*. The German Energy Society (Deutsche Gesellschaft für Sonnenenergie (DGS LV Berlin BRB). Earthscan, London&Sterling, VA (USA).
- [2] Machacek, J., Z. Prochazka, J. Drapela. 2009. The Temperature Dependant Efficiency of Photovoltaic Modules - a Long Term Evaluation of Experimental Measurements, *Renewable Energy*, T J Hammons (Ed.), InTech, WEB: <http://www.intechopen.com/books/>.
- [3] Markvart, T., L. Castaño. 2003. *Practical Handbook of Photovoltaics: Fundamentals and Applications*. Elsevier Ltd.

- [4] Skolopaki, E., J. A. Palyvos. 2009. On the temperature dependence of photovoltaic module electrical performance: A review of efficiency/power correlations. *Solar Energy*, issue 83, pp. 614-624.
- [5] Köhl, M. 2011. *From Climate Data to Accelerated Test Conditions*. Fraunhofer Institute for Solar Energy Systems, Freiburg, Germany, presented at the PVMRW, Golden (Colorado, USA), WEB: http://www1.eere.energy.gov/solar/pdfs/pvmrw2011_05_plen_kohl.pdf.
- [6] Коеv, К. 2011. Моделиране влиянието на някои фактори върху температурата на фотоволтаични модули. *Енергетика*, № 3, стр. 41-46.
- [7] Коеv, K., A. Krasteva, R. Ivanov. 2012. Potential of the renewable energy resources and their energy in Bulgaria. *Journal Ecology and Future* № 2, p. 3-14.
- [8] Nordmann, T., L. Clavadetscher. 2003. Understanding temperature effects on PV system performance. *Photovoltaic Energy Conversion*. Proceedings of 3rd World Conference (Volume 3), 18-18 May, Osaka, Japan, pp. 2243 – 2246.
- [9] Недев, Н., К. Коеv. 2012. Изследване производителността на фотоволтаични модули. В: *Научни трудове на Русенски университет “Ангел Кънчев”*, Русе, том 51, серия 3.1, стр. 35-39.
- [10] Коеv К., Н. Недев, К. Андонов, Кр. Мартев. 2011. Изследване влиянието на някои фактори върху производството на електрическа енергия от фотоволтаични модули. *Енергетика*, № 6, стр. 27-30.

REZULTATI ISPITIVANJA TEMPERATURE SOLARNIH MODULA

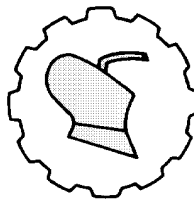
Konstantin Koev, Krasimir Martev

*Univerzitet “Angel Kančev”, Fakultet za elektroniku, elektrotehniku i automatizaciju,
Institut za električne pogone, Ruse, Bugarska*

Sazetak: Prikazani su rezultati istraživanja uticaja temperature stacionarnih fotonaponskih modula na proizvodnju energije. Moduli su povezani u grupe, sa ukupnim maksimalnim instalisanim kapacitetom od 117.24 kWp. Postavljeni su na krov zgrade u nenaseljenom području. Istraživanje je izvedeno tokom nekoliko tipičnih meseci, u periodu januar 2009 - decembar 2012. Proizvedena električna energija se menja u intervalu 0 - 25.55 kWh, za temperatursku razliku između fotonaponskih modula i okoline u intervalu od -5 do +30°C.

Ključne reči: fotonapski moduli, temperatura modula, električna energija, pregrevanje, hlađenje

Prijavljen: 29.07.2013.
Submitted:
 Ispravljen:
Revised:
 Prihvaćen: 07.10.2013.
Accepted:



UDK: 664.933

*Originalni naučni rad
Original scientific paper*

MODIFIED ATMOSPHERIC PACKAGING STRATEGIES TO PROLONG SHELF LIFE OF CHICKPEA (*Cicer arietinum L.*) SPROUTS

Ranjeet Singh^{1*}, Ashok Kumar², Sitaram D. Kulkarni¹

¹*Central Institute of Agricultural Engineering, Agro-Product Processing Division,
Nabi Bagh, Bhopal, India*

²*Department of Processing & Food Engineering, Punjab Agricultural University,
Ludhiana, India*

Abstract: The physicochemical and microbial changes in fresh chickpea sprouts during MA storage at 10°C temperatures and 75 % RH and ambient were examined by monitoring chickpea sprouts weight loss, pH, hypocotyl color changes, texture in terms of hardness, supported by overall visual quality evaluation and microbial infection by yeast and mold enumeration. Under MA storage, chickpea sprouts having different void volume in PP and LDPE polymeric films were stored for a week at 10°C temperature under MAP. In-pack gaseous composition was least in PP as compared with LDPE polymeric films. The PLW (%) was significantly lesser in 200g pack followed by 100; 150 g of sprouted chickpea samples packed PP films than those in LDPE polymeric film packs. Best hardness was maintained by 200g PP and 150g LDPE packaging treatment. Visual evaluation indicates that chickpea sprouts sample packed in 200g PP package received highest significant score. Yeast and mold growth appears to significantly contribute to microbial spoilage of chickpea sprouts, using modified atmosphere may restrict the spoilage problems caused by molds and yeast. Chickpea sprouts packed in Polypropylene (PP) was highly effective in maintaining the physic-textural and microbial analysis as evident by visual evaluation. The LDPE film package did not favorably affect the storage life of chickpea sprouts.

Key words: Chickpea, modified atmosphere packaging (MAP), Polypropylene (PP), low-density polyethylene (LDPE), microbial and visual quality parameters

* Corresponding author. E-mail: razi100@rediffmail.com

INTRODUCTION

Chickpea sprouts are the major seed sprouts in most Asian countries. Chickpea seeds can be stored for long periods of time and sprouts can be easily obtained by germinating the seeds in the dark for up to four days [10]. This process has been used by the Asian countries for centuries. Sprouts are a cheap source of certain vitamins in the diet and some vitamins are synthesized in the germinating seeds. The sprouting process results in an improvement in the vitamin content [6].

Though it is easy to grow sprout but the main drawback are shortage of time for sprouting as in most of the families both husband and wife are working. In western countries, china etc. sprouts are grown commercially and made available to consumers [2]. But in India the same trend has been started with the opening of food/vegetable malls. Sprouts are highly perishable in nature and get spoiled if not stored properly. Due to a short shelf life, sprouts are susceptible to get spoiled during distribution or in supermarket [12]. One of the primary causes of spoilage is visible mold growth and/or musty smell from the sprouts. Spoilage occurs sooner and more frequent when sprouts are not refrigerated in the supermarket and/or during distribution. Sprout can be easily bruised and readily infected with various bacteria, mold and yeast during handling and transportation. Sprouts cannot be stored for longer time under ambient conditions. So a method to increase the shelf life of sprout would be advantageous to producers as well as to the consumers and one of the options to increase the shelf life of sprouted chickpea is design and development of a suitable modified atmospheric packaging system. Keeping this in view the study is designed to extend the shelf life of sprouts using suitable polymeric films based on the modified atmosphere packaging under different storage condition.

MATERIAL AND METHODS

Plant Materials

The chickpea seeds (PBG-5) were washed and rinsed with $\text{Ca}(\text{OCl})_2$ at 20.000 ppm for 15 min for sterilization. The sterilized seeds were soaked in clean water (1: 3, w/v) for 12 h overnight at ambient room temperature. In the morning, the water is drained and the soaked seeds were rinsed with clean fresh water free from any contamination. The washed seeds (soaked) were then shifted to clean sterile muslin cloth and placed in dark at ambient temperature for sprout growth. After 36-48 h the sprouts were harvested for experimentation.

Measurement of In-pack Gaseous Composition

The in-pack gaseous composition measurement of sprouts was done as per the method adopted by Singh, 2012. A single hole covered with silicon septum was made in polymeric package for measurement of gas concentrations directly with gas analyzer (Model 902 D DualTrak O_2/CO_2 Analyzer, USA) at each day and gaseous composition O_2/CO_2 was recorded [3].

Physiological Loss in Weight (PLW)

The weight loss of chickpea sprout samples packed in *PP* and *LDPE* polymeric package under *MAP* and having 100, 150 and 200g weight was determined by weighing the individual package initially and on day of observation using a laboratory level weighing scale (Model CX 504, Scaltec Instruments GmbH, Germany) having least count 0.001g [4].

$$PLW (\%) = \frac{\text{Initial weight} - \text{Final weight}}{\text{Initial weight}} \times 100 \quad (1)$$

where,

PLW [%] - Physiological loss in weight.

pH Analysis

The sprouted chickpea mixture to measure pH was prepared [1] using 1:1 of product and distilled water. Ten grams of chickpea sprout mixture were blended for 2 min with 10 ml of distilled water (pH 7). Observation (pH) was then taken of the prepared mixture using a portable pH meter (H160G portable pH meter), which was antecedently calibrated using buffer solutions of pH 4 and 7. The pH of the freshly harvested sprouts was measured before packaging and later on each day of analysis from each of the 3 replicates of each treatment stored at 10°C temperature. Three samples per replicate were taken to measure pH.

Evaluation of Color Indices

The change in color can act as an analysis parameter to judge the freshness and quality of sprouted chickpea sprouts while storage [5]. The color of the sprouted chickpea was measured using a Hunter Lab Colorimeter (Miniscan XE plus, Hunter associates, USA) with "L", "a", "b" parameters. On each day of storage, the 'L', 'a' and 'b' values were noted using a Hunter Labscan (Model Miniscan XE plus, Hunter associates, USA). Color of the sprouts hypocotyl was measured on each day of analysis from each of the three replicates of each treatment stored at 10°C and control sample. The mean was taken for color indices.

Texture

Texture was determined as tenderness/hardness [7]. The freshly harvested sprouted chickpea sprouts are tender and, as they dry, out they become hard. As we were doing modified atmosphere packaging of the sprouts, we expected the sprouts to maintain the fresh, tenderness characteristic. Texture analysis was done on 10 fresh chickpea sprouts from each of the 3 replicates of each treatment stored at 10°C. The force necessary to compress the sprouts was measured using Texture Analyzer-Stable Micro System Model TA-XT2 (Hamilton, MA). The instrument was calibrated using the protocol provided by the manufacturer as discussed above before starting with the analysis.

Visual Quality

The visual quality evaluation was carried out for off odors of the sprout, discoloration, size of sprout and overall acceptance using a 10 point hedonic scale with the help of a test panel consisting of five panelists of different age groups and having different eating habits [8]. The sprouted chickpea was served raw and the average indices (*A.I.*) of all the panelists were computed for different samples.

$$A.I = \frac{\text{Total Scores}}{\text{No. of evaluators}} \quad (2)$$

Microbiological Analysis

Mold and yeast analysis for chickpea sprout samples in MA storage and control samples packed in *PP* and *LDPE* polymeric film, from each packaging modification during storage on day 0, 1, 2, 3, 4, 5, 6, and 7, was performed (USFDA 1999). Twenty-five g of each sample of serial dilutions were plated onto Potato Count Agar (PCA) which contained $100 \mu\text{g}\cdot\text{ml}^{-1}$ chloramphenicol (Sigma Chemical, St. Louis, Mo., U.S.A.), and were incubated in the dark for 5 d at room temperature. After incubation, mold and yeast colonies were counted with the assistance of a colony counter [10].

RESULTS AND DISCUSSION

In-pack Gaseous Composition

The average amount of in-pack headspace gaseous composition of oxygen (O_2) and carbon-dioxide (CO_2) for the safe storage of chickpea sprouts under MAP in perforated polymeric film *PP* and *LDPE* is shown in Fig. 1. It is clear from the Fig. 1 that the amount of head space gaseous composition decreased and remained unstable with duration of storage up-to 1st day and then maintained steady state thereafter. The effect of package weights on the gaseous concentration was clearly evident as these were varied between 21.60 to 15.63 %, 21.60 to 14.45 % and 21.60 to 12.15 % for O_2 and 0.03 to 8.59 %, 0.03 to 11.08 % and 0.03 to 14.19 for CO_2 in *PP* package having 100, 150 and 200 g of chickpea sprouts.

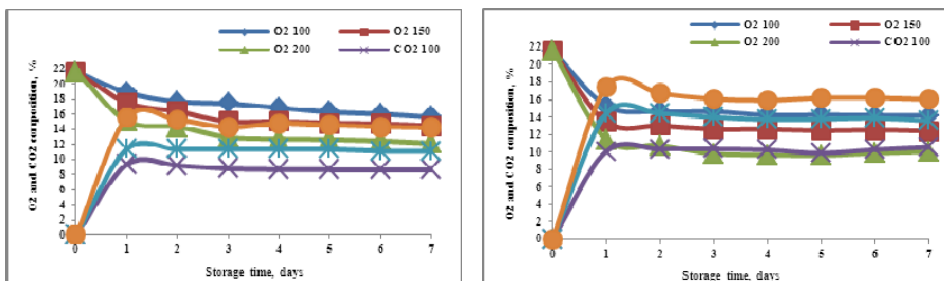


Figure 1. Package headspace gas composition (O_2/CO_2) storage under modified atmosphere

Similarly, the range for steady state headspace gas composition in *LDPE* package varied between 21.60 to 14.20 %, 21.60 to 12.39 % and 21.60 to 10.03 % for O₂ and 0.03 to 10.57 %, 0.03 to 13.57 % and 0.03 to 16.05 for CO₂ having package weight of 100, 150 and 200 g of chickpea sprouts. From this it is clear that in-pack gaseous composition was least in PP as compared with *LDPE* polymeric films. The effect of different weights on the gaseous composition was very much evident in both the PP and *LDPE* polymeric film package containing 100, 150 and 200 g of chickpea sprouts.

The headspace gas composition was found to be significant at 5 % level of significance ($p \leq 0.05$) influenced by all the factors including type of polymeric film, sample weight and duration of storage.

Physiological Loss in Weight (PLW)

The physiological loss in weight can be restored by bounding atmospheric storage temperature, relative humidity and also by using suitable designed package [9]. It is quite evident from Fig. 2 that the percent physiological loss in weight after 7th day of storage was comparatively lesser in PP film packages than in packages of *LDPE* polymeric films although the difference in mean values was significant. There was significant ($p \leq 0.05$) loss in weight was reported in initial values among the packaging films. *PLW* percentage increased at slow and steady rate with the duration of storage and rate of loss of weight. The *PLW* (%) was most in control sprout samples. However, the maximum weight loss was observed to be 0.982 % in *LDPE* 200g among all the polymeric film packages having different weights of chickpea sprouts. Sealed samples showed very marginal loss in weight as compared to unsealed control samples which recorded initial weight loss up to 6.49 % by the end of last day of storage period. It can be inferred from the trends that the *PLW* (%) was relatively lesser in 200g pack followed by 100; 150 g of sprouted chickpea samples packed and stored in PP films than those in *LDPE* polymeric film packs and the mean value difference was significant. Also, the effect of void volume showed significant effect on *PLW* (%) of sprouted samples sealed in different polymeric films.

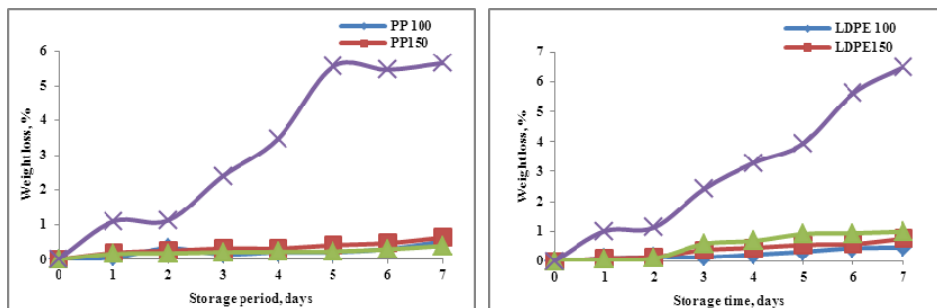


Figure 2. Physiological loss in weight (PLW) of chickpea sprout under modified atmosphere

pH of Sprouted Chickpea

The pH values of freshly packed chickpea sprout was alkaline in nature having pH value more than 7.0. It was observed that the pH value decline gradually in all the

packaging treatments during storage. The overall decline was much higher and rapid in *LDPE* film as compared with *PP* polymeric film. The cause behind decline in pH would be accumulation of more gaseous concentration inside the *LDPE* film causing increase in lactate content of packed sprouts during storage. The cause may be satisfying the low pH association with the accumulation of lactate and to a lesser extent of acetate [12] during sprouting. The effect on gaseous concentration caused due to different weight of the sample was very much evident having pH value observed to be 8.27, 8.25 and 8.55 on last day of storage in *PP* polymeric film. However, the pH of sprouted chickpea packed in *LDPE* was observed to be 7.85, 6.99 and 5.98 on last 7th day of storage in 100, 150 and 200 g package, respectively. A shift in pH value from alkaline to acidic (9.28 to 5.28) was observed in control sample packed in *LDPE* film (Fig 3). The cause clearly indicates that the lowering of pH was due to excessive and different gaseous composition developed inside the package containing different weight of chickpea sprout samples. The statistical analysis showed a significant difference between the means of pH value of *PP*, *LDPE* and control treatments ($p \leq 0.05$). The pH of the freshly harvested and packed chickpea sprout sample in *PP* and *LDPE* polymeric films sustain alkalinity in nature throughout the storage period.

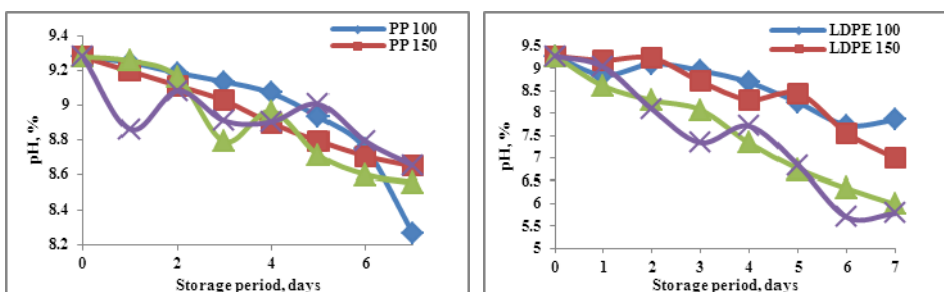


Figure 3. pH (%) content of chickpea sprouts under modified atmosphere

Color (L-value)

The hypocotyl color of chickpea sprouts is the important quality indices to determine the freshness of the product for greater acceptability and satisfactory purchase [11]. Deterioration in *L* value reflects loss in lightness of the sprouts and become off dated. The initial average '*L*' value of chickpea hypocotyl was 67.68. The average decrease in '*L*' value on 7th day of storage period was 38.50, 37.67 and 43.07 for *PP* package and 28.64, 32.59 and 38.57 for *LDPE* package containing 100, 150 and 200g of samples, respectively. The maximum hypocotyl color retention (Lightness) was observed in 200g *PP* package followed by 200g *LDPE* and 100g *PP* packages. The control sample showed poor off white color retention in both *PP* and *LDPE* package having 16.16 and 11.56 '*L*' value of hypocotyl, respectively. The significant decrease in '*L*' value indicated that control sample hypocotyl become darker as compared to other treatment over the entire storage period. It can be concluded that modified atmosphere packaging restore the darkening of the hypocotyl of chickpea sprout samples as well stored in *PP* and *LDPE* polymeric packs in different weights (Fig 4).

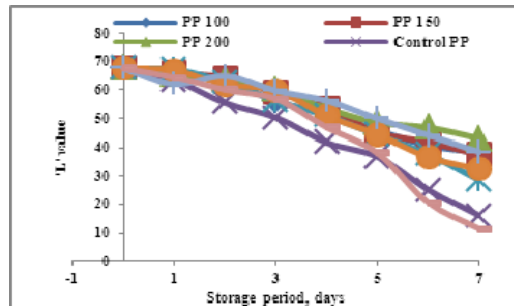


Figure 4. Hypocotyl color 'L' value of chickpea sprouts storage under modified atmosphere

Hardness

The maximum hardness of sprouted chickpea was observed 80.17 kgf on initial day of packaging for storage. A continues significant decline in texture in terms of hardness value of chickpea sprout was observed in all treatments as on 7th day of storage. The percent decline in hardness value was 16.68, 15.10 and 10.24 in PP packages containing 100, 150 and 200 g of sprouted chickpea, respectively on 7th day on modified storage. Similarly the decrease in hardness value was 24.80, 13.48 and 17.02 in LDPE packages containing 100, 150 and 200g of sprouted chickpea on 7th day on modified storage (Fig. 5).

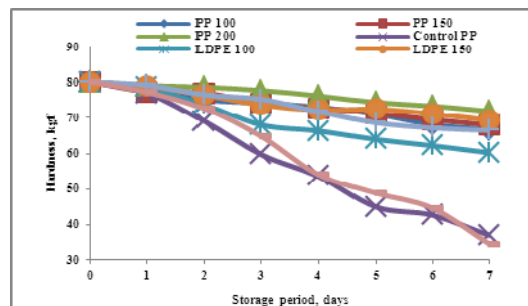


Figure 5. Hardness of chickpea sprouts storage under modified atmosphere at 10°C temperature and 75% relative humidity

Visual Quality

The mean visual score based on overall acceptance was observed maximum for 200g PP package followed by 150g PP and 150g LDPE packages during the storage period (Fig. 6). Both the controlled samples of PP and LDPE samples being exposed to air and had least overall scores followed by 200g and 100g LDPE package which indicates that chickpea sprouts sample packed in 200g PP package received highest significant sensory score. The optimal storage atmosphere observed based upon visual score was (O_2 6-7%; CO_2 9-10%) resulted in better maintenance of overall visual properties. The subjective and objective measures are in close agreement with each other.

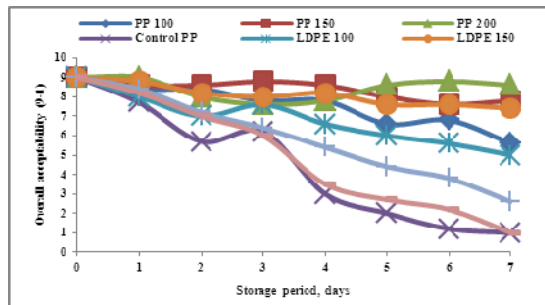


Figure 6. Overall acceptability value of chickpea sprouts under MAP Storage

Yeast and Mold

Mold and yeast counts of chickpea sprouts were variable during storage in the different packaging systems. The mold and yeast count of fresh sprouts were well below $1 \log_{10}$ CFU/g. The mold and yeast count was 3.37 , 4.22 and $2.03 \log_{10}$ CFU/g in PP package and 5.53 , 6.61 and $9.43 \log_{10}$ CFU/g in LDPE package in different treatments. Sprouts packaged in PP had significant increases ($P > 0.05$) in yeast and mold counts after 7 day of storage. It was also observed in sprouts packaged in PP package had no visible/physical signs of spoilage after 7 day of MAP storage having varied weight (Fig. 7). However, sprouts packed in LDPE packages had significant increases in amounts of yeast and molds during storage period. Conversely, sprouts in control samples had significantly more yeast and molds after the 7 days of storage period. In control sample the yeast and mold count of $38.61 \log_{10}$ CFU/g in PP and $52.01 \log_{10}$ CFU/g in LDPE package was observed on 7th day of storage. On day 2, control sprouts had small amounts of visible mold growth and a musty odor and after 4th day, both control samples had obvious physical signs of spoilage and unfit become for consumption. The yeast and mold counts in LDPE package were significantly higher than the counts on sprouts packaged in PP package because the gas composition inside the package may have reduced the presence of competitive micro-flora on the sprouts.

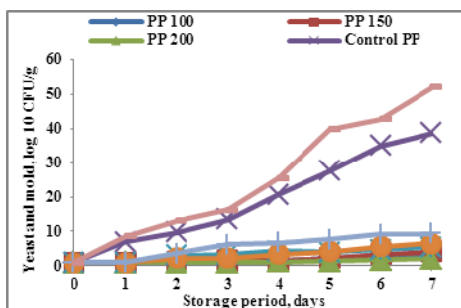


Figure 7. Yeast and mold enumeration of chickpea sprouts storage under modified atmosphere

Shelf-life of Chickpea Sprouts

Comparison of the most important characteristics of chickpea sprouts packed in polymeric film containing different weight of chickpea sprout were showed in Tab. 1. It is evident from the Tab. 1. that for both the subjective and objective measures of chickpea sprouts packed in *PP* film has better results as compared with *LDPE* packed samples having different void volume. The chickpea sprouts packed in 200g *PP* film was best followed by *PP* packed in 100g and 150g respectively. The chickpea sprouts packed in *PP* film packages were also brighter and firm without decay after 7 days of storage then the other treatments as it shown in Tab. 1.

Table 1. Comparison of the most important characteristics of chickpea sprouts packed in polymeric film containing different weight of chickpea sprout

MAP	Subjective measures					Objective measures (9-1)		
	HS Gas, (%)		PLW	pH	Hypocotyl Color	Hardness Better	Overall acceptability	Yeast and mold
	O ₂	CO ₂						
<i>PP</i> 100	15.63	8.59	Less	Alkaline	Better	Tender	Better	Less
<i>PP</i> 150	14.45	11.08	Less	Alkaline	Good	Tender	Good	Less
<i>PP</i> 200	12.15	14.19	Least	Alkaline	Best	Firm	Best	Least
<i>LDPE</i> 100	14.20	10.57	Less	Alkaline	Good	Tender	Better	Less
<i>LDPE</i> 150	12.39	14.43	More	Alkaline	Good	Tender	Good	More
<i>LDPE</i> 200	10.03	16.05	More	Acidic	Better	Tender	Good	More
Control	-	-	Most	Acidic	Bad	Soft	Bad	Most

CONCLUSIONS

Packaging of sprouts in *PP* film under *MAP* conditions was effective in maintaining the physico-textural and microbiological quality of produce. The sprouts package head space gaseous composition of 12.53 % O₂ and 14.19 % CO₂ was found suitable for shelf life extension in *PP* polymeric package. The fresh sprouts having pack size of 200g and lightness matching to L_h-value (color of hypocotyl) of 43 was successful in extending the postharvest life of chickpea sprouts for more than 7 days stored under modified atmosphere at 10°C temperature and 75% relative humidity with no development of off-odors. Subjective properties such as PLW, pH and color of sprout hypocotyls and hardness were suitably protected in *PP* polymeric packages and also received the highest objective measure of overall acceptability. The yeast and mold count on all *MAP* stored sprouts in *PP* and *LDPE* packaging increased during storage. However, in spite of marginal and significant increase, sprouts packed in *PP* film were effective in limiting yeast and mold growth.

BIBLIOGRAPHY

- [1] Barry-Ryan, C., O'Beirne, D. 1998. Effects of slicing method on the quality and storage-life of modified atmosphere packaged carrot discs. *Journal of Food Science*, 63 (5), 851 - 856.

- [2] Deepak, R. R., Shashi, P. 2007. Transient state in-pack respiration rates of mushroom under modified atmosphere packaging based on enzyme kinetics. *Postharvest Technology*, 98 (12), 319-326.
- [3] Del, M. A., Baiano, A. 2006. Respiration rate of minimally processed lettuce as affected by packaging. *Journal of Food Engineering*, 74 (19), 60-69.
- [4] Lee, D. S., Heggar, P. E., Lee, J., Yam, K. L. 1991. Model for fresh produce respiration in modified atmospheres based upon the principle of enzyme kinetics. *Journal of Food Science*, 56, 1580-1585.
- [5] Lee, D. S., Song, Y., Yam, K. L. 1996. Application of an enzyme kinetics based respiration model to permeable system experiment of fresh produce. *Journal of Food Engineering*, 27(3), 297-310.
- [6] Magaram, M. F., Stotts, C. L., Chen, T. S., Smith, C. H., Kirsch, A. J. 1985. Folacin content of alfalfa and mung bean sprouts: the effect of extraction procedures and maturity. *Journal Sci Food Agri*. 36, 1155-60.
- [7] McLaughlin, C. P., Beirne, D. 1999. Respiration rate of a dry coleslaw mix as affected by storage temperature and respiratory gas concentrations. *Journal of Food Science*, 64, 116-119.
- [8] Ranganna, S. 1977. *Manual of Analysis of Fruit and Vegetable Products*. Tata -McGraw-Hill, New Delhi, USA.
- [9] Rocculi, P., Del, M. A., Romani, S. 2006. Use a simple mathematical model to evaluate dipping and MAP effects on aerobic respiration of minimally processed apples. *Journal of Food Engineering*, 76 (34), 334-340.
- [10] Soylemez, G., Brashears, M. M., Smith, D. A., Cuppett, S. L. 2001. Microbial quality of alfalfa seeds and sprouts after a chlorine treatment and packaging modifications. *Journal of Food Science*, 66 (1), 153-157.
- [11] Susanna, C. F., Fernanda, A. R., Jeffrey, K. B. 2002. Modeling respiration rate of fresh fruits and vegetables for modified atmosphere packages: a review, *Journal of Food Engineering*, 52, 99–119.
- [12] Singh, R. 2012. *Design, evaluation and modeling of chickpea sprouts in modified atmosphere packaging*. PhD Thesis, PAU, Ludhiana.

**POSTUPCI PAKOVANJA U MODIFIKOVANOJ ATMOSVERI
RADI PRODUŽENJA VREMENA SKLADIŠTENJA
KLICA LEBLEBIJA (*Cicer arietinum L.*)**

Ranjeet Singh¹, Ashok Kumar², Sitaram D. Kulkarni¹

1 Centralni institut za poljoprivrednu tehniku, Odsek za preradu poljoprivrednih proizvoda, Nabi Bagh, Bhopal, India

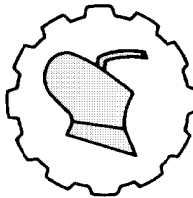
2 Poljoprivredni Univerzitet Punjab, Institut za preradu i inženjeringu prehrambenih proizvoda, Ludhiana, Punjab, India

Sažetak: Fiziko-hemiske i mikrobiološke promene na svežim klicama leblebija tokom MA skladištenja na temperaturi od 10°C i vlažnosti od 75 % su ispitivane praćenjem gubitka mase, pH, promene boje i tvrdoće, uz opštu vizuelnu procenu

kvaliteta i mikrobiološke infekcije brojem kvasaca i plesni. Klice leblebija različitih zapremina su držane u *PP* i *LDPE* polimer filmovima sedam dana na 10°C u MAP uslovima. Sastav gasova u pakovanju je bio najmanji u *PP* u poređenju sa *LDPE* polimer filmovima. *PLW (%)* je značajno niža u pakovanjima od 200g, 100g i 150g (redom) od *PP* filma nego onih u pakovanju od *LDPE* filma. Tvrdoća je najbolje očuvana kod pakovanja 200g *PP* i 150g *LDPE*. Vizuelnom procenom najbolji rezultat je dobio uzorak iz pakovanja 200g *PP*. Porast kvasaca i plesni značajno doprinosi mikrobiološkom kvarenju klica, a upotreba modifikovane atmosvere može da redukuje ove efekte. Pakovanje od polipropilena (*PP*) veoma efikasno je održavalo fizičke i mikrobiološke osobine i teksturu klica, što je i vizuelno potvrđeno. *LDPE* pakovanje nije značajno uticalo na smanjenje vremena skladištenja klica leblebija.

Ključne reči: Leblebije, modifikovana atmosvera pakovanja (MAP), polipropilen (*PP*), polietilen male gustine (*LDPE*), mikrobiološki i vizuelni parametri kvaliteta

Prijavljen: 12.8.2013
Submitted:
Ispravljen:
Revised:
Prihvaćen: 10.03.2014.
Accepted:



UDK: 622.244

*Originalni naučni rad
Original scientific paper*

INSIDE OVERPRESSURE UTILIZATION FOR A STABILITY INCREASING AT THE THIN-WALLED ROTATIONAL SYMMETRICAL SHELL STRAINED BY AXIAL FORCE

Stanislav Kotšmíd*, Marián Minárik

*Technical University in Zvolen, Faculty of Environmental and Manufacturing
Technology, Department of Mechanics and Mechanical Engineering,
Zvolen, Slovak Republic*

Abstract: The members, strained by axial force, are used in the different areas of human activities. If members have a big slenderness, it can to origin a problem with losing of their stability. One of the possibilities, how can be partially eliminated this deficiency with not extending its parameters and of course its mass, is adding of force effects, which will be operate against to force effects making of stability losing. The article deals with theoretical possibility of stability increasing by adding of inside overpressure. It describes allocation and interaction of effected stresses according to the appropriate formulas and solves concrete sample. Last but not least, it shows graphical layout of effect stresses and satisfaction of stability condition with regard to different values of inside overpressure and geometrical parameters of members. The article brings a possible way of members stability increasing and in case of experimental verification we can predict favourable future of this.

Key words: buckling, stability, shell, overpressure

INTRODUCTION

The straining of members by axial force is often occurred in the different industrial machines in agriculture, forestry, architecture and engineering. In the practice, the engineers effort to create members with a small mass and a high carrying capacity, so it directs to making a slender struts, which can succumb losing of the shape stability under

* Corresponding author. E-mail: stanislav.kotsmid@gmail.com

axial force loading. Losing of stability is a status of strut, where are created conditions for solid transition from stable to unstable position, when this transition is characterised by changing of solid shape.

While the value of force, which causes the pressure stress in the strut, is not higher than critical value, which is dependent on the strut connecting, the strut is straight and it is strained on pressure only. If the critical value is exceeded, deformation of the strut increases until its destruction. This critical value is called critical buckling force, which characterises losing of stability.

By this value can be solved critical stress in struts. In depending on connecting condition, geometrical parameters and strut material, this stress can be much less than the yield value, so material is not utilized in sufficient degree. Here is created question, how can be increased utilization of strut, if we do not want to extend its geometrical parameters and its mass of course. We assume, one of the way is adding of the force effect, which will be operate against to force effect making pressure.

MATERIAL AND METHODS

There can be determined critical buckling force for prismatic, centric pressured strut by procedure, which was elaborated by Leonhard Euler. If we suppose homogeneity material of the strut and unlimited validity of the Hook law, the strut is stable and has straight shape at small axial force.

If this axial force achieves critical value, the strut is in indifferent balance and it stays in new deformed shape with bended axis (Fig. 1) [1, 3, 6, 7].

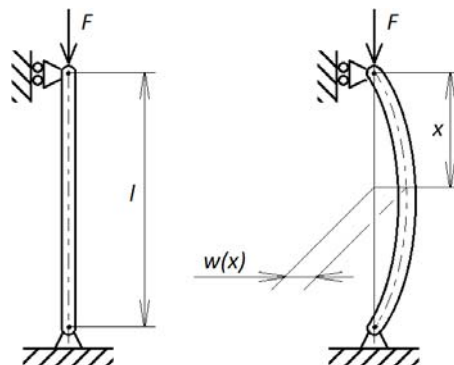


Figure 1. Deformation of the strut by axial force F

The computing of critical buckling force can be deduced by procedure, which is described in literature [6]. Final formula for computing of this force is:

$$F_{krit} = \frac{n^2 \cdot \pi^2 \cdot E \cdot J_{min}}{(\beta \cdot l)^2} \quad (1)$$

Where:

- | | | |
|-----|-------------|--|
| n | [\cdot] | - constant, which determines shape of bended line, |
| E | [Pa] | - Young modulus of elasticity, |

J_{min}	[m ⁴]	- minimum quadratic moment of strut cross section,
β	[-]	- buckling coefficient,
l	[m]	- length of strut.

The critical stress in strut is computed as:

$$\sigma_{krit} = \frac{F_{krit}}{A} \quad (2)$$

Where:

A [m²] - cross section area.

Let investigate, what will happen, if strut, constructed as shell, is strained by inside overpressure except axial force (Fig. 2).

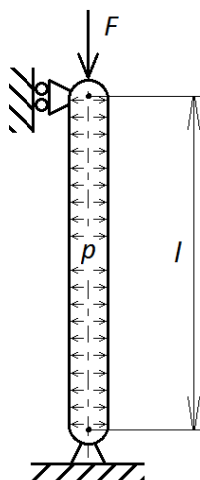


Figure 2. The shell strained by axial force and inside overpressure

At the shells (ratio of the inside diameter and the wall thickness is smaller than 0.1) as members of the planar character, can be used a membrane theory for computing in some cases. This theory ignores effect of bending and torsion moments, and feed and contact force, so it makes solution of problem easier [1, 4, 5].

For using of this theory must be met next conditions. Geometrical parameters of the shell (thickness, radius of curvature, centre of curvature) must be changed continuously. Alone forces, which strain of the shell, must operate in contact plane to middle surface. Straining of the shell does not have to be changed suddenly. Connecting of the shell must be statically determinate. If any from these rules is not right, it can cause bending and torsion moments there, what makes solution of task harder [1, 4, 6].

In the shell can be created three planes through some point P ; the contact plane to middle surface, the meridian plane in which is situated axis of symmetry and plane, which is perpendicular on previous two. Let extract infinity small element near to point P (Fig. 3) [2, 3, 6].

In the places of element operate only normal stresses σ_m and σ_t . If inside overpressure p operates there, condition of static at the element balance in direction of the normal n to middle surface has form:

$$p \cdot ds_m \cdot ds_t - 2 \cdot \sigma_m \cdot h \cdot ds_t \cdot \sin \frac{d\vartheta_m}{2} - 2 \cdot \sigma_t \cdot h \cdot ds_m \cdot \sin \frac{d\vartheta_t}{2} = 0 \quad (3)$$

Where:

p	[Pa]	- inside overpressure in the shell,
h	[m]	- thickness of the wall,
σ_m	[Pa]	- meridian stress,
σ_t	[Pa]	- tangent stress,
ds_m	[m]	- element height,
ds_t	[m]	- element width,
d_m	[°]	- angle of element curvature in meridian direction,
d_t	[°]	- angle of element curvature in tangent direction,
ρ_m	[m]	- radius of element curvature in meridian direction,
ρ_t	[m]	- radius of element curvature in tangent direction.

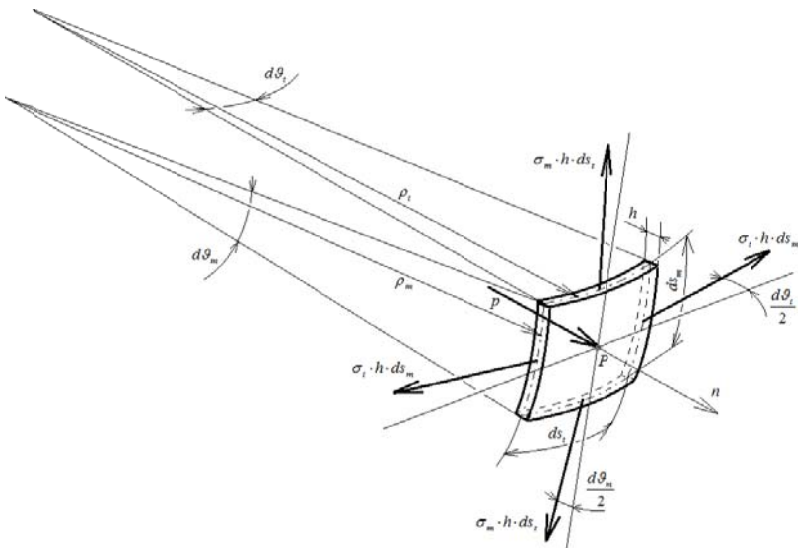


Figure 3. Element of the shell

After putting and removing of the special part in formula we get Laplace formula:

$$\frac{\sigma_m}{\rho_m} + \frac{\sigma_t}{\rho_t} = \frac{p}{h} \quad (4)$$

This formula gives relation among tangent stress σ_t , meridian stress σ_m , inside overpressure p and geometrical parameters h , ρ_m and ρ_t .

Next needed formula for solution is condition of equilibrium for part of the shell, which is cutting by the plane, perpendicular on the axis of rotation.

$$\sum F_{ix} = 0 \quad p \cdot \pi \cdot r^2 - 2 \cdot \sigma_m \cdot \pi \cdot r \cdot h = 0 \quad (5)$$

Where:

r [m] - shell radius.

After putting $\rho_t = r$ and $\rho_m = \infty$ we get for σ_m and σ_t formulas:

$$\sigma_t = \frac{p \cdot r}{h} \quad (6)$$

$$\sigma_m = \frac{p \cdot r}{2 \cdot h} \quad (7)$$

This theory predicts operating of stresses in tangent and meridian direction, what is stress operated in the shell axial direction. It is tensile stress and wants to stretch the shell in axial direction. As we have written, axial force causes compression stress. Both stresses operate in the same direction and in the same plane so they can be algebraic summed up and from this sum and tangent stress can be made up reduce stress according to one of the strength theories. There can be different results of this sum. If there will be zero compression stress, only meridian stress will be operate in axial direction. If there will be compression stress equal to meridian stress, no stress will be operate in axial direction. If there will be compression stress higher than meridian stress, pressure will be operate in axial direction and after exceeding of the critical value, losing of stability come soon. So stability condition can have this form:

$$\sigma_m - \sigma_{tl} + \sigma_{krit} > 0 \quad (8)$$

Where:

σ_{tl} [Pa] - compression stress caused by axial force F .

For computing of reduce stress can be used theory HMH. Formula has next form

$$\sigma_{red}^{HMH} = \sqrt{(\sigma_m - \sigma_d)^2 + \sigma_t^2 - (\sigma_m - \sigma_d) \cdot \sigma_t} \quad (9)$$

On the basic of previous ideas, let solve next task, where will be investigated the shape stability of pipe strained by axial force. Pipe will be strained by force $F = 5\,000$ N, on the both ends will be connected by a joint and will have outside diameter $D = 17$ mm, wall thickness $h = 1$ mm and length $l = 1$ m. Material of pipe is chosen with yield value $R_e = 180$ MPa and safety coefficient $k = 2$.

We can use Euler formula (1) and formulas for computing of critical buckling and compression stress.

$$F_{krit} = \frac{1^2 \cdot \pi^2 \cdot 2,1 \cdot 10^{11} \cdot \frac{\pi \cdot (0,017^4 - 0,015^4)}{64}}{(1 \cdot 1)^2} = 3346,82N$$

$$\sigma_{krit} = \frac{3346,82}{\frac{\pi \cdot (0,017^2 - 0,015^2)}{4}} = 66,58MPa$$

$$\sigma_{tl} = \frac{5000}{\pi \cdot (0,017^2 - 0,015^2)} = 99,47 \text{ MPa}$$

4

Next we add the inside overpressure in pipe $p = 10 \text{ MPa}$. Then tangent and meridian stresses have values:

$$\sigma_t = \frac{10 \cdot 8}{1} = 80 \text{ MPa}$$

$$\sigma_m = \frac{10 \cdot 8}{2 \cdot 1} = 40 \text{ MPa}$$

According to formula (8) for stability condition we get:

$$40 - 99,47 + 66,58 = 7,11 > 0$$

what means, there is no losing of stability. Reduce stress has value:

$$\sigma_{red}^{HMH} = \sqrt{(40 - 99,47)^2 + 80^2 - (40 - 99,47) \cdot 80} = 72 \text{ MPa}$$

RESULTS AND DISCUSSION

As we can see from computed values in previous part, computed F_{krit} is smaller than axial force F . According to this, the pipe can lose its stability. Compression stress is higher than critical buckling stress too. Pipe does not meet stability condition.

Table 1. Dependence of stresses and stability condition of pipe according to the inside overpressure value

$p \text{ (MPa)}$	$\sigma_m \text{ (MPa)}$	$\sigma_t \text{ (MPa)}$	$\sigma_{tl} \text{ (MPa)}$	$\sigma_{red} \text{ (MPa)}$	$\sigma_m - \sigma_{tl} + \sigma_{krit} \text{ (MPa)}$
0	0	0	99,47	99,47	-32,89
1	4	8		91,73	-28,89
2	8	16		84,61	-24,89
3	12	24		78,28	-20,89
4	16	32		72,94	-16,89
5	20	40		68,83	-12,89
6	24	48		66,16	-8,89
7	28	56		65,13	-4,89
8	32	64		65,80	-0,89
9	36	72		68,14	3,11
10	40	80		71,97	7,11
11	44	88		77,07	11,11
12	48	96		83,21	15,11
13	52	104		90,18	19,11

With straining of pipe by inside overpressure was created meridian stress in the wall, which operates against to compression stress. The pipe after application meets stability condition and reduce stress is smaller than permissible stress too. *Table 1* shows

how these stresses and stability condition are changed according to value of inside overpressure.

From this table we can see that under value 8 MPa of inside overpressure, last column is negative. It means inside overpressure is too small for compensation of the pressure caused by axial force F . Only when value is equals 8.22 MPa, it can be met stability condition. When there are higher values of inside overpressure, stability condition is met. There is meridian stress still smaller than compression stress caused by axial force F .

From the table we can see that values of reduce stress reaches permissible stress before value 13 MPa of inside overpressure, but meridian stress is still smaller than compression stress. It is caused by increasing of tangent stress. It brings idea that inside overpressure cannot be increased without control.

Fig. 4 shows activity of stresses in pipe and fact, that we get the smallest reduce stress, when inside overpressure is on the limit of stability.

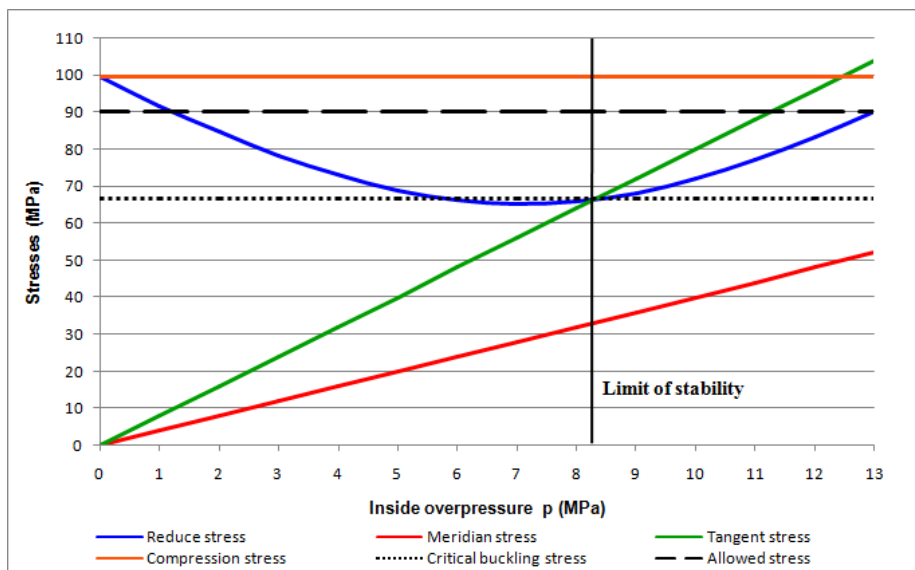


Figure 4. Dependence of stresses according to the inside overpressure changing

Fig. 5 shows, how reduce stress in the pipe is changed according to inside overpressure and outside diameter. In this case can be said, with decreasing of inside overpressure is needed increasing of geometrical parameters for decreasing of reduce stress, and inside out.

Fig. 6 shows to meet stability condition according to pipe outside diameter and inside overpressure changing. We can see, at value of outside diameter 15 mm is all interval of stability values for inside overpressure 0 – 15 MPa in negative values. It means, any shown value of inside overpressure do not compensate compressive stress for no losing of stability. On the other hand, in value of outside diameter 20 mm is all values in positive interval, so inside overpressure is not needed there, but it can help to

decreasing of reduce stress. From this we can bring idea, with increasing of pipe outside diameter is needed smaller inside overpressure to stability safety.

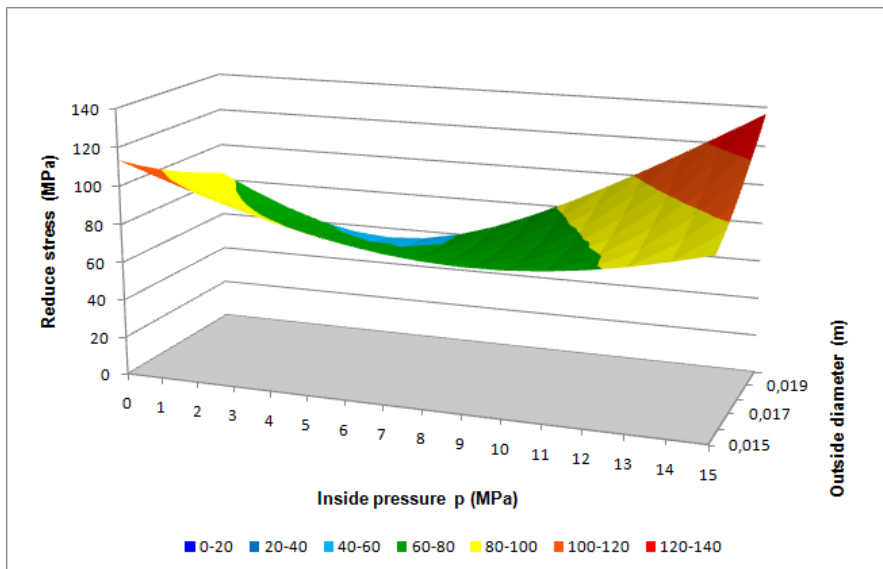


Figure 5. Dependence of reduce tension according to pipe diameter and inside overpressure changing

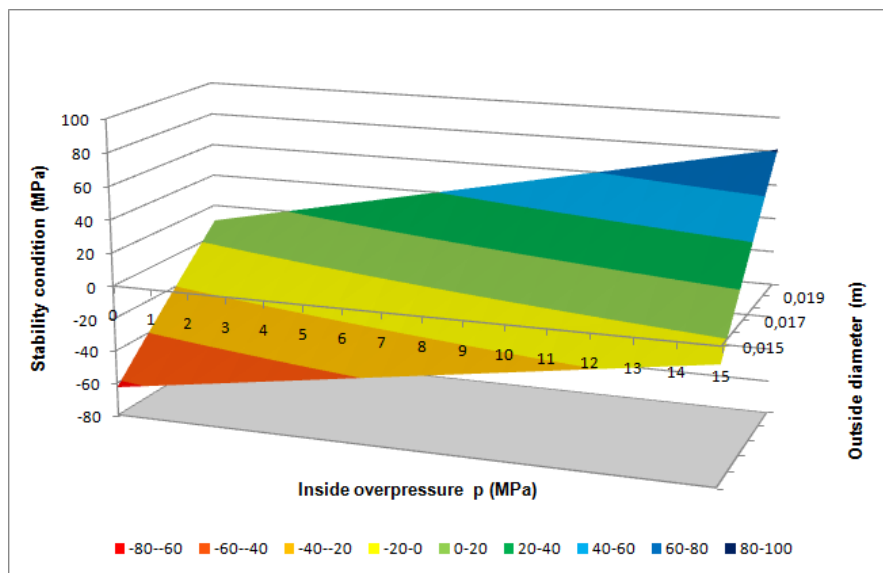


Figure 6. Dependence of meet condition according to pipe outside diameter and inside overpressure changing

CONCLUSIONS

In the present, when the utilization of materials is increased, research and development is oriented on new materials like the composites. Yield value of materials and of course their utilization can be increased by suitable structure and constitution of materials. The next way is to better know the character and the straining of forces and create the way, how these force effects can be partially eliminated by their allocation, or adding of force effects which will operate in the opposite direction.

In the article is shown elimination of origin force effects by adding of another force effects operated in opposite direction. Computation shows, that this way can have invocation in future. Except of experimental verification, there will have to be solved another aspects for implementation of this way to the practise.

One of the aspects is the shape of heads and technology of their connecting. In a pressure vessels is often used a plate circular head, which is welded to the shell. This simple solution causes existence of superior stress, so there might be create relieve by means a race around all circuit and thickness of the head might be higher than thickness of the shell.

The next aspect is an assurance of the clear membrane state in inside forces, what means the assurance of necessary deformation and static equilibrium only through membrane forces. In the practise it means to solve suitable location. At last but not least will be necessary to see on safety at escape of inside overpressure from the pipe.

We suppose that after solving previous aspects, this way of material efficiency increasing can have favourable future.

BIBLIOGRAPHY

- [1] Bischoff, M., Bletzinger, K. U., Wall, W. A., Ramm, E. 2004. *Models and finite elements for thin-walled structures* In: *Encyclopedia of computational mechanics*. USA: John Wiley & Sons, Inc.
- [2] Bodnár, F., Minárik, M. 2009. *Pružnosť a pevnosť II*. Zvolen: Technická univerzita vo Zvolene.
- [3] Hájek, E., Reif, P., Valenta, F. 1988. *Pružnosť a pevnosť I*. Praha: SNTL.
- [4] Riley, W. F., Struges, L. D. 1993. *Engineering mechanics – Statics I*. USA: John Wiley & Sons, Inc.
- [5] Schafer, B. 2002. Local, distortional, and Euler buckling of thin-walled columns. *Journal of structural engineering*. Volume 128. Issue 3. 10 pages.
- [6] Trebuňa, F., Jurica, V., Šimčák, F. 2000. *Pružnosť a pevnosť II*. Košice: Vienala.
- [7] Trebuňa, F., Šimčák, F. 1999. *Tenkostenné nosné prvky a konštrukcie*. Košice: Vienala.

UPOTREBA UNUTRAŠNJEG NADPRITISKA ZA POVEĆANJE STABILNOSTI TANKOG ZIDA ROTACIONE SIMETRIČNE OPLATE OPTEREĆENE AKSIJALNOM SILOM

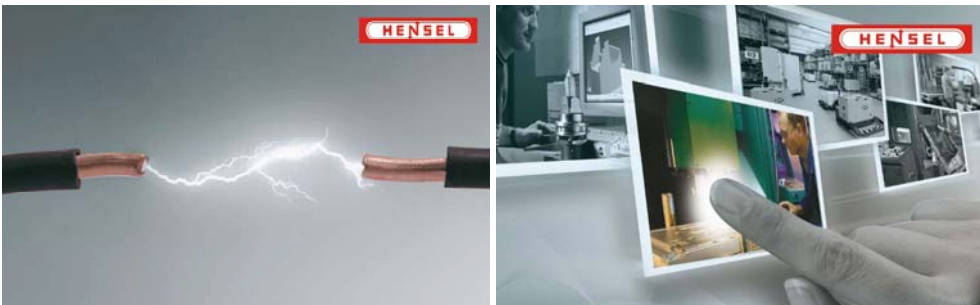
Stanislav Kotšmíd, Marián Minárik

Tehnički univerzitet u Zvolenu, Fakultet za životnu sredinu proizvodnu tehnologiju,
Institut za mehaniku i mašinstvo, Zvolen, Republika Slovačka

Sažetak: Elementi, opterećeni aksijalnom silom, se koriste u raznim oblastima. Ako su savitljivi, mogu izgubiti svoju stabilnost. Jedna od mogućnosti za delimično otklanjanje ovog nedostatka, bez ojačavanja i povećanja mase, je dodavanje sile koja će delovati suprotno tako da uravnoteži opterećeni element. Ovaj rad obrađuje teorijsku mogućnost povećanja stabilnosti dodavanjem unutrašnjeg nadpritiska. Opisan je položaj i interakcija opterećenja odgovarajućim jednačinama i dobijeno rešenje konkretnog problema. Pokazan je i grafički prikaz dobijenog efekta i zadovoljenje uslova stabilnosti u odnosu na različite vrednosti unutrašnjeg nadpritiska i geometrijskih parametara elemenata. U radu je dat i poseban način povećanja stabilnosti elemenata i eksperimentalne verifikacije daljih postupaka.

Ključne reči: izvijanje, stabilnost, oplata, nadpritisak

Prijavljen: 15.08.2013.
Submitted:
Ispravljen:
Revised:
Prihvaćen: 12.02.2014.
Accepted:



MILUROVIĆ KOMERC
Uglovac, Beogradsko 32, Tel: 011/949-324, Fax: 011/949-899
www.milurovickomerc.com



DRAGO PROJEKT



ITALIJANSKI
ČASOVI, KURSEVI
KONVERZACIJA
PRIPREMA ISPITA

Jovan Jovanović
064 84 23 696
063 84 23 696
www.itluoinsegnante.net

Velbek

Postojimo zbog Vas
Veleprodaja i distribucija pića

омладинска задрушка
ГРАДАЦ

11070 Нови Београд, Бул. др Јордана Јинђића 179
дом КУЛТУРЕ - СТУДЕНТСКИ ГРАД
телеф/факс: 011/2673-244



Agencija za prevodilačke
i konsultantske usluge
"LINGUAES MUNDI"
www.linguamundi.com
E-mail: office@linguamundi.com
linguamundi@eunet.rs
Tel. (011) 3240 737, 3342 166, 3342 237
Faks (011) 3228 315
Mobilni 063 8043 519

Vaša najpouzdanija veza sa svetom!



ZEMUN, Slobodana Bajića 23
tel./faks 011/37-54-079, mob. 063/84-99-101
e-mail:akademskiizdanja@gmail.com



Vlada Republike Srbije
Ministarstvo prosvete, nauke i
tehnološkog razvoja

CIP – Каталогизација у публикацији
Народна библиотека Србије, Београд

631(059)

ПОЉОПРИВРЕДНА техника : научни часопис =
Agricultural engineering : scientific journal / главни и
одговорни уредник Горан Тописировић. – Год. 1, бр. 1
(1963)- . - Београд; Земун : Институт за пољопривредну
технику, 1963- (Београд : Штампарија "Академска
издања") . – 25 cm

Тромесечно. – Прекид у излажењу
од 1987-1997. године

ISSN 0554-5587 = Пољопривредна техника
COBISS.SR-ID 16398594